# DISCONTINUOUS GALERKIN METHODS FOR WEAKLY COUPLED HYPERBOLIC MULTI-DOMAIN PROBLEMS

QINGYUAN LIU†, CHI-WANG SHU‡, AND MENGPING ZHANG§

**Abstract.** In this paper, we develop and analyze the Runge-Kutta discontinuous Galerkin (RKDG) method to solve weakly coupled hyperbolic multi-domain problems. Such problems involve transfer type boundary conditions with discontinuous fluxes between different domains, calling for special techniques to prove stability of the RKDG methods. We prove both stability and error estimates for our RKDG methods on simple models, and then apply them to a biological cell proliferation model [18]. Numerical results are provided to illustrate the good behavior of our RKDG methods.

**Key words.** RKDG scheme, multi-domain problems, discontinuous fluxes, biological cell proliferation model

**AMS subject classifications.** 65M12, 65M60, 92-08

## 1. Introduction.

This paper is dedicated to the study of hyperbolic multi-domain problems with a transfer type discontinuous flux communication between domains. The generic setup below (detailed in [2]) covers a broad range of coupling problems which have received considerable attention over the past decade. Let $\Omega \subset \mathbb{R}^n$, $n \geq 1$, be a simply connected open set and $\{\Omega_i\}_{i=1,\cdots,\mathcal{N}}$ a nonoverlapping collection of open subsets of $\Omega$ with $\cup_{i=1}^{\mathcal{N}} \overline{\Omega_i} = \overline{\Omega}$. Then consider the phase space $\mathcal{K} \subset \mathbb{R}^F$ with integer $F \geq 1$, a convex open set. For a given $T > 0$, the problem reads as follows: find $\phi : [0,T] \times \Omega \to \mathcal{K}$ solution of

$$\begin{aligned}
\partial_t \phi + div(f_i(\mathbf{x},\phi)) &= S_i(\mathbf{x},\phi), \quad on \quad (0,T) \times \Omega_i \quad i = 1, \cdots, \mathcal{N}, \\
\phi(0,\mathbf{x}) &= \phi_0(\mathbf{x}), \quad on \quad \Omega, \\
\phi(t,\mathbf{x}) &= 0, \quad on \quad (0,T) \times \partial\Omega, \\
\psi_{i,j}(\phi(t,\mathbf{x}^-)) &= \phi(t,\mathbf{x}^+), \quad on \quad (0,T) \times \overline{\Omega_i} \cap \overline{\Omega_j},
\end{aligned}$$

where $f_i : \Omega_i \times \mathcal{K} \to \mathbb{R}^{n \times F}$ and $S_i : \Omega_i \times \mathcal{K} \to \mathbb{R}^F$ are smooth functions. The last equation models the transmission condition between any pair of adjacent open sets $\Omega_i$ and $\Omega_j$ such that $\overline{\Omega_i} \cap \overline{\Omega_j} \neq \emptyset$ for $(i,j) \in \{1, \cdots, \mathcal{N}\}^2$. The transmission condition, that is discontinuous flux communication, is prescribed thanks to the smooth function $\psi_{i,j} : \mathcal{K} \to \mathcal{K}$ which allows us to define the right-hand trace of $\phi(t,\mathbf{x}^+)$ at $\overline{\Omega_i} \cap \overline{\Omega_j}$ from the left-hand trace $\phi(t,\mathbf{x}^-)$.

Multi-domain problems have a wide range of applications, including the biological model of cell proliferation [2], which is our main interest in this paper and will be detailed in the third section. Other applications include multiphase flow in porous media [3], traffic flow with discontinuous road surface conditions [6], and sedimentation in thickener-clarifier units [5] as examples. In all these models, the mathematical difficulty lies in proving the well-posedness of the initial boundary value problems (IBVP), and this is summarized well in the review [4].

†School of Mathematical Sciences, University of Science and Technology of China, Hefei, Anhui 230026, P.R. China. E-mail: qyliu@mail.ustc.edu.cn.

‡Division of Applied Mathematics, Brown University, Providence, RI 02912, U.S.A. E-mail: shu@dam.brown.edu. Research is supported in part by AFOSR grant F49550-12-1-0399 and NSF grant DMS-1418750.

§School of Mathematical Sciences, University of Science and Technology of China, Hefei, Anhui 230026, P.R. China. E-mail: mpzhang@ustc.edu.cn. Research supported by NSFC grant 11471305.

In this paper we deal with a nonconservative coupling setting where the velocities are nonlocal. As highlighted later in this paper, these two mathematical features arise naturally in a biological context. We address the model developed in [18] in the general context of cell dynamics, describing the time evolution of a density function depending on the age and maturity variables. This unknown is governed by a kinetic-like equation involving velocities that are functions of integro-moments of the unknown and the age and maturity variables. Closure equations for these velocities are naturally discontinuous in the age and maturity variables, precisely at the biological checkpoints which correspond to the interfaces between the biological phases [26]. These discontinuities require additional information which are handled as local double IBVPs, where inner boundary conditions are formulated to express the biological switch.

More details on the biological background of the model will be provided in section 3, which is devoted to its mathematical analysis and its numerical approximation. The theoretical study of this model has been performed in [24]. The main difficulties come from the nonlocal velocity, the coupling between boundary conditions, and the vector nature of the coupling problem. We will pay special attention to the construction and analysis of stable and high order accurate numerical algorithms for this model, which to our knowledge has not been addressed in two-dimensional ($2D$) simulations for nonconservative coupling. Although the well-posedness issue is not handled with the same mathematical tools as that in [24], the numerical methods that we have designed in this paper can be used in the application contexts cited above, like, for instance, the traffic models [23].

The numerical algorithm we develop and analyze in this paper is the class of high order accurate explicit Runge-Kutta discontinuous Galerkin (RKDG) methods. As we will see below, such methods are particularly suited for handling the transfer type discontinuous flux communication inter-domain boundary conditions. Discontinuous Galerkin (DG) method is a class of finite element methods using completely discontinuous basis functions, which are usually chosen as piecewise polynomials. The use of a DG discretization in space gives the methods the high-order accuracy, the flexibility in handling complicated geometries, and easiness in treating boundary conditions, which is important for the multi-domain model studied in this paper. The DG method was originally developed in 1973 by Reed and Hill [22] to solve the framework of neutron transport, that is a time independent linear hyperbolic equation. A major development of the DG method was carried out by Cockburn et al in a series of papers [7, 9, 10, 11, 12], in which they have established a framework to easily solve nonlinear time dependent problems, such as the Euler equations of gas dynamics, using explicit, nonlinearly stable high order Runge-Kutta time discretizations [25, 19] (the most popular scheme in this class is the third order strong-stability-preserving (SSP) Runge-Kutta method that we use in this paper), and DG discretization in space, with exact or approximate Riemann solvers as interface fluxes and total variation bounded (TVB) nonlinear limiters to achieve non-oscillatory properties for strong shocks. The RKDG method has advantages of high-order accuracy, high parallel efficiency and the flexibility in handling complicated geometry. Stability and convergence results for the RKDG method applied to scalar conservation laws are given in [27, 28]. In this paper, in order to avoid the technical complication for analyzing fully discrete RKDG schemes, we will perform stability and convergence analysis only for the semi-discrete DG scheme, and concentrate on the difficulty in handling the particular inter-domain boundary conditions in the analysis.

The remainder of this paper is organized into three sections. In section 2, we describe the main idea of our algorithm and analysis on a simple model of transport equation in just one domain in one and two dimensions. The transfer type discontinuous flux communication is realized through the interaction from the right boundary of the domain to the left boundary. We analyze the well-posedness of this model problem and the stability and convergence of the corresponding DG scheme. The idea of this analysis is used later in the proof for the more complicated biological model. We also demonstrate the result using two numerical examples in this section. In section 3, we focus on the biological model describing the cell dynamics in developing ovarian follicles [18]. Following the procedure of analysis in section 2, we present the proof of well-posedness for the problem and stability for our DG scheme. Numerical validation is performed in the last part of this section which demonstrates that this scheme can be used to solve this model well. Section 4 contains concluding remarks which summarize the results in this paper and discuss possible future work.

## 2. A simple model with the main ideas.

**2.1. One-dimensional case.** In this section, we will consider the following problem with suitable initial conditions

$$\begin{cases} u_t + u_x = 0, & x \in [0,1] \\ u(0,t) = Au(1,t) \end{cases} \tag{2.1}$$

wherein the factor $A$ in the transfer type boundary condition is an arbitrary number not equal to one (for our application, we have $A > 1$ which will be assumed in the discussion below). Even though this is a one-domain problem, the transfer type discontinuous flux communication is realized through the interaction from the right boundary of the domain to the left boundary.

**2.1.1. Well-posedness.** First, we will discuss the well-posedness of the problem. We multiply the partial differential equation in (2.1) by $(1+k_0x)u(x,t)$ and then integrate it on [0,1], wherein the positive parameter $k_0$ is yet to be determined:

$$\begin{aligned} 0 &= \int_0^1 (1+k_0x)u_tu + (1+k_0x)u_xu dx \\ &= \int_0^1 (1+k_0x)\left(\tfrac{1}{2}u^2\right)_t dx + \int_0^1 (1+k_0x)\left(\tfrac{1}{2}u^2\right)_x dx \\ &= \tfrac{1}{2}\tfrac{d}{dt}\int_0^1 (1+k_0x)u^2dx + \tfrac{1}{2}[(1+k_0x)u^2]\,|_0^1 - \tfrac{k_0}{2}\int_0^1 u^2dx. \end{aligned}$$

We would like to control the second term involving boundary values to be non-negative. Considering the specific boundary condition, we should take $k_0$ such that $k_0 \geq A^2 - 1$, so that

$$[(1+k_0x)u^2]\,|_0^1 = [(1+k_0)u^2(1,t) - u^2(0,t)] \geq 0.$$

Specially, we can choose $k_0 = A^2 - 1 > 0$, thus,

$$\frac{d}{dt}\int_0^1 (1+k_0x)u^2dx \;=\; k_0\int_0^1 u^2dx \;\leq\; k_0\int_0^1 (1+k_0x)u^2dx.$$

Using the Gronwall inequality we can deduce that

$$\int_0^1 (1+k_0x)u^2(x,t)dx \leq \mathrm{e}^{k_0t}\int_0^1 (1+k_0x)u^2(x,0)dx. \tag{2.2}$$

Notice that this weighted norm is equivalent to standard $L^2$ norm $\|u\|_{L^2}$, hence the problem is well-posed under the standard $L^2$ norm for finite time as well.

**2.1.2. Stability for the semi-discrete DG scheme.** Next, we will discuss the semi-discrete DG scheme for this model and its stability. In the subsequent subsections, without loss of generality, we choose $A = 2$ to simplify the discussion. We define

$$0 = x_{\frac{1}{2}} < x_{\frac{3}{2}} < \cdots < x_{n+\frac{1}{2}} = 1, \quad I_j = [x_{j-\frac{1}{2}}, x_{j+\frac{1}{2}}],$$
$$h_j = x_{j+\frac{1}{2}} - x_{j-\frac{1}{2}}, \quad h = \max_j h_j, \quad V_h = \{v : v\,|_{I_j} \in P^k(I_j)\},$$

where $P^k(I_j)$ denotes the set of polynomials defined on $I_j$ of degree at most $k$. We will consider uniform mesh $h_j = h$ for simplicity, although this restriction is not necessary for our algorithm or the analysis below.

The semi-discrete DG scheme can be defined as follows. Find $u_h \in V_h$ such that, for all $v_h \in V_h$ we have

(2.3)
$$\begin{cases} \int_{I_j} (u_h)_t v_h dx - \int_{I_j} u_h (v_h)_x dx + \widehat{u}_{j+\frac{1}{2}} (v_h)^-_{j+\frac{1}{2}} - \widehat{u}_{j-\frac{1}{2}} (v_h)^+_{j-\frac{1}{2}} = 0, \quad j = 1, 2, \cdots, n, \\ \widehat{u}_{j+\frac{1}{2}} = (u_h)^-_{j+\frac{1}{2}}, \quad j = 1, 2, \cdots, n, \quad \widehat{u}_{\frac{1}{2}} = 2\widehat{u}_{n+\frac{1}{2}}. \end{cases}$$

Notice that the transfer type boundary condition is easy to implement in our DG scheme.

**Proposition 1.** *The DG scheme (2.3) is stable for fixed time t,*

$$\|u_h(\cdot, t)\|_{L^2([0,1])} \le M_0 \|u_h(\cdot, 0)\|_{L^2([0,1])}, \tag{2.4}$$

*where $M_0$ is a constant which may depend on t.*

*Proof.* In order to prove the stability of the DG scheme (2.3), we would like to follow the lines of the proof for the well-posedness and would like to take our test function $v_h$ as $w = (1 + k_0 x)u_h$. Here we choose $k_0 = A^2 - 1 = 3$. Unfortunately, $w$, being a polynomial of one degree higher, is not in our finite element space $V_h$, so the best we could do is to take its projection in $V_h$. We will use the standard $L^2$ projection $P$, which is defined as the unique piecewise polynomial $Pw$ in $V_h$ satisfying

$$\int_{I_j} (w - Pw)\phi dx = 0, \qquad \forall \phi \in P^k(I_j). \tag{2.5}$$

In the interval $I_j$, $u_h \in P^k(I_j)$. Let $\xi = \frac{2(x - x_j)}{h} \in [-1, 1]$. Let $P_l(\xi)$ be the standard Legendre polynomial of degree $l$, and $Q_l(\xi) = \sqrt{\frac{2l+1}{2}} P_l(\xi)$. From the properties of standard Legendre polynomials, we can get the following properties for $Q_l$

$$\begin{aligned} & Q_l(-1) = \sqrt{\tfrac{2l+1}{2}}(-1)^l, \quad l = 0, 1, \cdots, k+1 \\ & \int_{-1}^{1} Q_l Q_s d\xi = \delta_{ls}, \quad l, s \le k+1 \\ & \xi Q_l(\xi) = \sqrt{\tfrac{(l+1)^2}{(2l+1)(2l+3)}} Q_{l+1}(\xi) + \sqrt{\tfrac{l^2}{(2l-1)(2l+1)}} Q_{l-1}(\xi), \quad l = 1, 2, \cdots, k. \end{aligned} \tag{2.6}$$

We will first prove the following useful lemma.

LEMMA 2.1. *Let $v(\xi)$ is a polynomial of degree at most k about $\xi$, written as $v(\xi) = \sum_{s=0}^{k} b_s Q_s(\xi)$, where the coefficients $\{b_s\}_{s=0,\cdots,k}$ are independent of $\xi$. If $g(\xi) = (c_0 + c_1\xi)v(\xi)$, wherein $c_0$ and $c_1$ are constants, and $\epsilon_g = g - Pg$, then we have*

$$\epsilon_g = c_1 b_k \sqrt{\frac{(k+1)^2}{(2k+1)(2k+3)}} Q_{k+1}(\xi). \tag{2.7}$$

*Proof.* Since $g \in P^{k+1}$, we can express $g(\xi)$ under the basis $Q_s(\xi)_{s=1}^{k+1}$ as

$$\begin{aligned} g(\xi) &= \sum_{s=0}^{k}(c_0+c_1\xi)b_sQ_s(\xi) = \sum_{s=0}^{k} d_sQ_s(\xi) + c_1b_k\xi Q_k(\xi) \\ &= \sum_{s=0}^{k} a_sQ_s(\xi) + c_1b_k\sqrt{\tfrac{(k+1)^2}{(2k+1)(2k+3)}}Q_{k+1}(\xi), \end{aligned}$$

where $\{d_s\}_{s=0,\cdots,k}$ and $\{a_s\}_{s=0,\cdots,k}$ can be written out explicitly in terms of $\{b_s\}_{s=0,\cdots,k}$, but such explicit expression is not needed in the analysis below. Here the last property in (2.6) is used. Under these notations, we have

$$\epsilon_g = c_1b_k\sqrt{\frac{(k+1)^2}{(2k+1)(2k+3)}}Q_{k+1}(\xi).$$

□

For any fixed time $t$, we can express our DG solution $u_h$ on $I_j$ by the basis $Q_s(\xi)$ with coefficients $b_s^j$ as below

$$u_h(x,t) = \sum_{s=0}^{k} b_s^jQ_s(\xi), \qquad x \in I_j,$$

here we omit $t$ in the coefficients $b_s^j$. In the interval $I_j$,

$$w = (1+3x)u_h(x,t) = \left((1+3x_j) + \frac{3h}{2}\xi\right)u_h(x,t).$$

Thus, with Lemma 2.1, we have

$$\epsilon = w - Pw = \frac{3h}{2}b_k^j\sqrt{\frac{(k+1)^2}{(2k+1)(2k+3)}}Q_{k+1}(\xi). \tag{2.8}$$

Taking $v_h = Pw \in V_h$ in the scheme (2.3), we have

$$\int_{I_j}(u_h)_tPwdx - \int_{I_j}u_h(Pw)_xdx + \widehat{u}_{j+\frac{1}{2}}(Pw)^-_{j+\frac{1}{2}} - \widehat{u}_{j-\frac{1}{2}}(Pw)^+_{j-\frac{1}{2}} = 0. \tag{2.9}$$

Noticing the property of the projection in (2.5), and since $u_h \in P^k(I_j)$, $(u_h)_x \in P^k(I_j)$, we have

$$\begin{gathered} \textstyle\int_{I_j}(u_h)_tPwdx = \int_{I_j}(u_h)_twdx, \\ \textstyle\int_{I_j}u_h(Pw)_xdx = (u_h)^-_{j+\frac{1}{2}}(Pw)^-_{j+\frac{1}{2}} - (u_h)^+_{j-\frac{1}{2}}(Pw)^+_{j-\frac{1}{2}} - \int_{I_j}(u_h)_xwdx. \end{gathered}$$

From equation (2.9), we can deduce that

$$\begin{aligned} 0 = {} & \textstyle\int_{I_j}(u_h)_twdx - (u_h)^-_{j+\frac{1}{2}}(Pw)^-_{j+\frac{1}{2}} + (u_h)^+_{j-\frac{1}{2}}(Pw)^+_{j-\frac{1}{2}} \\ & + \textstyle\int_{I_j}(u_h)_xwdx + \widehat{u}_{j+\frac{1}{2}}(Pw)^-_{j+\frac{1}{2}} - \widehat{u}_{j-\frac{1}{2}}(Pw)^+_{j-\frac{1}{2}} \\ = {} & \textstyle\int_{I_j}(u_h)_twdx + \int_{I_j}(u_h)_xwdx + \left((u_h)^+_{j-\frac{1}{2}} - \widehat{u}_{j-\frac{1}{2}}\right)(Pw)^+_{j-\frac{1}{2}} \end{aligned}$$

Substituting the expression of $w$, and noticing that

$$\begin{aligned} \textstyle\int_{I_j}(u_h)_twdx &= \tfrac{1}{2}\tfrac{d}{dt}\textstyle\int_{I_j}(1+3x)u_h^2dx, \\ \textstyle\int_{I_j}(u_h)_xwdx &= \textstyle\int_{I_j}(1+3x)(u_h)_xu_hdx = \int_{I_j}(1+3x)\left(\tfrac{1}{2}u_h^2\right)_xdx \\ &= \tfrac{1}{2}(u_h^2)^-_{j+\frac{1}{2}}(1+3x_{j+\frac{1}{2}}) - \tfrac{1}{2}(u_h^2)^+_{j-\frac{1}{2}}(1+3x_{j-\frac{1}{2}}) - \tfrac{3}{2}\textstyle\int_{I_j}u_h^2dx, \end{aligned}$$

we have

$$\begin{aligned} 0 = \quad & \tfrac{1}{2}\tfrac{d}{dt}\int_{I_j}(1+3x)u_h^2dx - \tfrac{3}{2}\int_{I_j}u_h^2dx + \tfrac{1}{2}(u_h^2)^-_{j+\frac{1}{2}}(1+3x_{j+\frac{1}{2}}) - \tfrac{1}{2}(u_h^2)^+_{j-\frac{1}{2}}(1+3x_{j-\frac{1}{2}}) \\ & + \left((u_h)^+_{j-\frac{1}{2}} - \widehat{u}_{j-\frac{1}{2}}\right)(Pw)^+_{j-\frac{1}{2}}. \end{aligned}$$

Summing from $j=1$ to $n$, then we have

$$\begin{aligned} 0 \quad & = \tfrac{1}{2}\tfrac{d}{dt}\int_0^1(1+3x)u_h^2dx - \tfrac{3}{2}\int_0^1 u_h^2dx + \tfrac{1}{2}\sum_{j=1}^n(u_h^2)^-_{j+\frac{1}{2}}(1+3x_{j+\frac{1}{2}}) \\ & \quad -\tfrac{1}{2}\sum_{j=1}^n(u_h^2)^+_{j-\frac{1}{2}}(1+3x_{j-\frac{1}{2}}) + \sum_{j=1}^n\left((u_h)^+_{j-\frac{1}{2}} - \widehat{u}_{j-\frac{1}{2}}\right)(Pw)^+_{j-\frac{1}{2}}. \end{aligned} \tag{2.10}$$

Considering the boundary condition $\widehat{u}_{\frac{1}{2}} = 2\widehat{u}_{n+\frac{1}{2}} = 2(u_h)^-_{n+\frac{1}{2}}$, we have

$$\sum_{j=1}^n(u_h^2)^-_{j+\frac{1}{2}}(1+3x_{j+\frac{1}{2}}) = \sum_{j=1}^{n-1}\widehat{u}^2_{j+\frac{1}{2}}(1+3x_{j+\frac{1}{2}}) + \widehat{u}^2_{\frac{1}{2}} = \sum_{j=1}^n\widehat{u}^2_{j-\frac{1}{2}}(1+3x_{j-\frac{1}{2}}).$$

Because $Pw = w - \epsilon$, the last term in equation (2.10) can be written as

$$\left((u_h)^+_{j-\frac{1}{2}} - \widehat{u}_{j-\frac{1}{2}}\right)(Pw)^+_{j-\frac{1}{2}} = \left((u_h)^+_{j-\frac{1}{2}} - \widehat{u}_{j-\frac{1}{2}}\right)(w)^+_{j-\frac{1}{2}} - \left((u_h)^+_{j-\frac{1}{2}} - \widehat{u}_{j-\frac{1}{2}}\right)(\epsilon)^+_{j-\frac{1}{2}},$$

wherein

$$\left((u_h)^+_{j-\frac{1}{2}} - \widehat{u}_{j-\frac{1}{2}}\right)(w)^+_{j-\frac{1}{2}} = (u_h^2)^+_{j-\frac{1}{2}}(1+3x_{j-\frac{1}{2}}) - (u_h)^+_{j-\frac{1}{2}}\widehat{u}_{j-\frac{1}{2}}(1+3x_{j-\frac{1}{2}}).$$

Now equation (2.10) becomes

$$\begin{aligned} 0 = \quad & \tfrac{1}{2}\tfrac{d}{dt}\int_0^1(1+3x)u_h^2dx - \tfrac{3}{2}\int_0^1 u_h^2dx + \tfrac{1}{2}\sum_{j=1}^n\widehat{u}^2_{j-\frac{1}{2}}(1+3x_{j-\frac{1}{2}}) \\ & -\tfrac{1}{2}\sum_{j=1}^n(u_h^2)^+_{j-\frac{1}{2}}(1+3x_{j-\frac{1}{2}}) + \sum_{j=1}^n(u_h^2)^+_{j-\frac{1}{2}}(1+3x_{j-\frac{1}{2}}) \\ & - \sum_{j=1}^n(u_h)^+_{j-\frac{1}{2}}\widehat{u}_{j-\frac{1}{2}}(1+3x_{j-\frac{1}{2}}) - \sum_{j=1}^n\left((u_h)^+_{j-\frac{1}{2}} - \widehat{u}_{j-\frac{1}{2}}\right)(\epsilon)^+_{j-\frac{1}{2}} \\ = \quad & \tfrac{1}{2}\tfrac{d}{dt}\int_0^1(1+3x)u_h^2dx - \tfrac{3}{2}\int_0^1 u_h^2dx + \tfrac{1}{2}\sum_{j=1}^n\left((u_h)^+_{j-\frac{1}{2}} - \widehat{u}_{j-\frac{1}{2}}\right)^2(1+3x_{j-\frac{1}{2}}) \\ & - \sum_{j=1}^n\left((u_h)^+_{j-\frac{1}{2}} - \widehat{u}_{j-\frac{1}{2}}\right)(\epsilon)^+_{j-\frac{1}{2}}. \end{aligned} \tag{2.11}$$

Therefore, we have

$$\begin{aligned} & \tfrac{1}{2}\tfrac{d}{dt}\int_0^1(1+3x)u_h^2dx - \tfrac{3}{2}\int_0^1 u_h^2dx \\ = \quad & -\tfrac{1}{2}\sum_{j=1}^n\left((u_h)^+_{j-\frac{1}{2}} - \widehat{u}_{j-\frac{1}{2}}\right)^2(1+3x_{j-\frac{1}{2}}) + \sum_{j=1}^n\left((u_h)^+_{j-\frac{1}{2}} - \widehat{u}_{j-\frac{1}{2}}\right)(\epsilon)^+_{j-\frac{1}{2}} \\ \le \quad & -\tfrac{1}{2}\sum_{j=1}^n\left((u_h)^+_{j-\frac{1}{2}} - \widehat{u}_{j-\frac{1}{2}}\right)^2(1+3x_{j-\frac{1}{2}}) + \tfrac{1}{2}\sum_{j=1}^n\left(\left((u_h)^+_{j-\frac{1}{2}} - \widehat{u}_{j-\frac{1}{2}}\right)^2 + \left((\epsilon)^+_{j-\frac{1}{2}}\right)^2\right) \\ \le \quad & \tfrac{1}{2}\sum_{j=1}^n\left((\epsilon)^+_{j-\frac{1}{2}}\right)^2. \end{aligned} \tag{2.12}$$

With the properties in (2.6), using the expression of $\epsilon$ in (2.8), and noticing that

$$\int_{I_j}u_h^2dx = \frac{h}{2}\int_{-1}^1\left(\sum_{s=0}^k b_s^jQ_s(\xi)\right)^2d\xi = \frac{h}{2}\sum_{s=0}^k(b_s^j)^2 \ge \frac{h}{2}(b_k^j)^2,$$

we have

$$\begin{aligned} \left((\epsilon)^+_{j-\frac{1}{2}}\right)^2 = \quad & \tfrac{9h^2}{4}(b_k^j)^2\tfrac{(k+1)^2}{(2k+1)(2k+3)}Q_{k+1}^2(-1) \\ = \quad & \tfrac{9h^2}{8}\tfrac{(k+1)^2}{2k+1}(b_k^j)^2 \le \tfrac{9h}{4}\tfrac{(k+1)^2}{2k+1}\int_{I_j}u_h^2dx. \end{aligned}$$

Let $C_k = \frac{9(k+1)^2}{4(2k+1)}$, which is a constant only depending on the polynomial degree $k$, then (2.12) gives us

(2.13)
$$\frac{d}{dt}\int_0^1 (1+3x)u_h^2 dx \le 3\int_0^1 u_h^2 dx + \sum_{j=1}^n C_k h \int_{I_j} u_h^2 dx \le (3+C_k h)\int_0^1 (1+3x)u_h^2 dx.$$

Similarly as before, from the Gronwall inequality and the equivalence of the two norms, we reach the conclusion that the semi-discrete DG scheme is stable under the standard $L^2$ norm for fixed time.

□

**2.1.3. Convergence for the semi-discrete DG scheme.** We now consider the error estimate for the DG scheme defined in equation (2.3).

**Proposition 2.** *The solution $u_h$ of the DG scheme (2.3) for the problem (2.1) with a sufficiently smooth solution $u$ which is in the Sobolev space $H^{k+1}([0,1])$ satisfies the following error estimate*

$$\|(u-u_h)(\cdot,t)\|_{L^2([0,1])} \le C_0 h^{k+1}, \tag{2.14}$$

*where $C_0$ depends on $u$ and its derivatives but is independent of $h$.*

*Proof.* For the exact solution $u$, we also have

(2.15)
$$\begin{cases} \int_{I_j} u_t v_h dx - \int_{I_j} u(v_h)_x dx + \widehat{u}_{j+\frac12}(v_h)^-_{j+\frac12} - \widehat{u}_{j-\frac12}(v_h)^+_{j-\frac12} = 0, \quad j = 1,2,\cdots,n, \quad \forall v_h \in V_h \\ \widehat{u}_{j+\frac12} = (u)^-_{j+\frac12} = (u)^+_{j+\frac12}, \quad j = 1,2,\cdots,n-1, \quad \widehat{u}_{n+\frac12} = (u)^-_{n+\frac12}, \quad \widehat{u}_{\frac12} = (u)^+_{\frac12} = 2\widehat{u}_{n+\frac12}. \end{cases}$$

Let $e = u - u_h$ denote the error. Subtract equation (2.3) from (2.15), then we can get the error equation

(2.16)
$$\begin{cases} \int_{I_j} e_t v_h dx - \int_{I_j} e(v_h)_x dx + \widehat{e}_{j+\frac12}(v_h)^-_{j+\frac12} - \widehat{e}_{j-\frac12}(v_h)^+_{j-\frac12} = 0, \quad j = 1,2,\cdots,n, \quad \forall v_h \in V_h \\ \widehat{e}_{j+\frac12} = (e)^-_{j+\frac12}, \quad j = 1,2,\cdots,n, \quad \widehat{e}_{\frac12} = 2\widehat{e}_{n+\frac12}. \end{cases}$$

We now decompose the error as $e_h = u_h - P^- u$ and $\varepsilon_h = u - P^- u$, wherein $P^-$ is the Gauss-Radau projection onto $P^k(I_j)$ (see for example [8, 16]), which has following properties. For each interval $I_j$, we have

$$\int_{I_j} \varepsilon_h v_h dx = 0, \ \forall v_h \in P^{k-1}(I_j); \quad (\varepsilon_h)^-_{j+\frac12} = 0. \tag{2.17}$$

Standard approximation theory [13] implies, for a smooth function $u$, the error estimate $\|\varepsilon_h\| \le Ch^{k+1}$, where here and below $C$ denotes a constant which may depends on the exact solution $u$ and its derivatives, and on time $t$, but is independent of the mesh size $h$. $C$ can take a different value in each occurrence.

Substituting $e = \varepsilon_h - e_h$ into equation (2.16), we can obtain that

(2.18)
$$\begin{aligned} & \int_{I_j}(e_h)_t v_h dx - \int_{I_j} e_h(v_h)_x dx + (\widehat{e_h})_{j+\frac12}(v_h)^-_{j+\frac12} - (\widehat{e_h})_{j-\frac12}(v_h)^+_{j-\frac12} \\ = \ & \int_{I_j}(\varepsilon_h)_t v_h dx - \int_{I_j} \varepsilon_h(v_h)_x dx + (\widehat{\varepsilon_h})_{j+\frac12}(v_h)^-_{j+\frac12} - (\widehat{\varepsilon_h})_{j-\frac12}(v_h)^+_{j-\frac12}, \quad \forall v_h \in V_h, \end{aligned}$$

wherein

$$\begin{aligned} &(\widehat{e_h})_{j+\frac12} = (e_h)^-_{j+\frac12}, \quad j = 1,2,\cdots,n, \quad (\widehat{e_h})_{\frac12} = 2(\widehat{e_h})_{n+\frac12}, \\ &(\widehat{\varepsilon_h})_{j+\frac12} = (\varepsilon_h)^-_{j+\frac12}, \quad j = 1,2,\cdots,n, \quad (\widehat{\varepsilon_h})_{\frac12} = 2(\widehat{\varepsilon_h})_{n+\frac12}. \end{aligned}$$

Owing to (2.17), the right hand side of equation (2.18) can be written as

$$RHS_j = \int_{I_j} (\varepsilon_h)_t v_h dx.$$

Let $w = (1+3x)e_h$, and $P$ be the $L^2$ projection which project $w$ onto $P^k$. Taking $v_h = Pw$, and using the same approach as in the proof of stability, we can rewrite the left hand side of equation (2.18) as

$$\begin{aligned} LHS_j = \; & \textstyle\int_{I_j} (e_h)_t w dx + \frac{1}{2}(e_h^2)^-_{j+\frac{1}{2}}(1+3x_{j+\frac{1}{2}}) - \frac{1}{2}(e_h^2)^+_{j-\frac{1}{2}}(1+3x_{j-\frac{1}{2}}) \\ & \textstyle -\frac{3}{2}\int_{I_j} e_h^2 dx + \left((e_h)^+_{j-\frac{1}{2}} - (\widehat{e_h})_{j-\frac{1}{2}}\right)(Pw)^+_{j-\frac{1}{2}}. \end{aligned}$$

Let $[e_h]_{j-\frac{1}{2}} = (e_h)^+_{j-\frac{1}{2}} - (\widehat{e_h})_{j-\frac{1}{2}}, j = 1, 2, \cdots, n$. Substituting $Pw = w - \epsilon$ and summing up over $j$, we can get that

$$\sum_{j=1}^{n} LHS_j = \frac{1}{2}\frac{d}{dt}\int_0^1 (1+3x)e_h^2 dx - \frac{3}{2}\int_0^1 e_h^2 dx + \frac{1}{2}\sum_{j=1}^{n}[e_h]^2_{j-\frac{1}{2}}(1+3x_{j-\frac{1}{2}}) - \sum_{j=1}^{n}[e_h]_{j-\frac{1}{2}}(\epsilon)^+_{j-\frac{1}{2}}.$$

Similar to the discussion in the stability analysis, we have

$$\sum_{j=1}^{n} LHS_j \geq \frac{1}{2}\left(\frac{d}{dt}\int_0^1 (1+3x)e_h^2 dx - (3+C_k h)\int_0^1 e_h^2 dx\right).$$

Recalling the approximation property of the Gauss-Radau projection, if $u$ is smooth enough, then

$$\int_0^1 (\varepsilon_h)_t Pw dx \leq Ch^{k+1}\|Pw\|_{L^2},$$

From equation (2.18), we can obtain

$$\begin{aligned} & \textstyle\frac{1}{2}\left(\frac{d}{dt}\int_0^1 (1+3x)e_h^2 dx - (3+C_k h)\int_0^1 e_h^2 dx\right) \leq \int_0^1 (\varepsilon_h)_t Pw dx \\ \leq \; & \textstyle Ch^{k+1}\left(\int_0^1 (Pw)^2 dx\right)^{\frac{1}{2}} \leq Ch^{k+1}\left(\int_0^1 w^2 dx\right)^{\frac{1}{2}} \\ \leq \; & \textstyle Ch^{2k+2} + \frac{C}{4}\int_0^1 (1+3x)^2 e_h^2 dx \leq Ch^{2k+2} + C\int_0^1 (1+3x)e_h^2 dx. \end{aligned}$$

Let $C_1 = 3 + C_k + 2C$, we have

$$\frac{1}{2}\frac{d}{dt}\int_0^1 (1+3x)e_h^2 dx \leq Ch^{2k+2} + C_1\int_0^1 (1+3x)e_h^2 dx. \tag{2.19}$$

Using Gronwall inequality, we have

$$\int_0^1 (1+3x)e_h^2(x,t)dx \leq Ch^{2k+2} + \mathrm{e}^{C_1 t}\int_0^1 (1+3x)e_h^2(x,0)dx.$$

Choosing a suitable initial condition as $u_h(\cdot,0)$ which can make $\int_0^1 e_h^2(x,0)dx$ proportional to $h^{2k+2}$ or even equal to 0, we have

$$\int_0^1 e_h^2(x,t)dx \leq \int_0^1 (1+3x)e_h^2(x,t)dx \leq Ch^{2k+2}.$$

Hence we achieve the optimal $L^2$ error estimate

$$\|(u-u_h)(\cdot,t)\|_{L^2([0,1])} \leq C_0 h^{k+1}. \tag{2.20}$$

□

**2.1.4. Numerical example. Example 1.** We test the following problem

$$\begin{cases} u_t + u_x = -\frac{1}{2}\sin(2\pi(x-t)), & x, y \in [0,1], \\ u(0,t) = 2u(1,t) \end{cases}$$

which has the exact solution $u(x,t) = \sin(2\pi(x-t))(1-\frac{1}{2}x)$. Using our scheme with $P^2$ elements and third order time discretization, we get the errors and orders of accuracy in Table 2.1. Clearly, the numerical result coincides with the conclusion of our analysis.

TABLE 2.1
*error table,* $t = 0.5$, $cfl = 0.2$

| $N$ | $L^1$-err | $L^1$-ord | $L^2$-err | $L^2$-ord | $L^\infty$-err | $L^\infty$-ord |
|---|---|---|---|---|---|---|
| 20 | 6.82E-05 | – | 9.23E-05 | – | 4.97E-04 | – |
| 40 | 8.47E-06 | 3.01 | 1.16E-05 | 3.00 | 6.45E-05 | 2.94 |
| 80 | 1.06E-06 | 3.00 | 1.45E-06 | 3.00 | 8.20E-06 | 2.98 |
| 160 | 1.32E-07 | 3.00 | 1.81E-07 | 3.00 | 1.03E-06 | 2.99 |
| 320 | 1.65E-08 | 3.00 | 2.26E-08 | 3.00 | 1.30E-07 | 2.99 |
| 640 | 2.06E-09 | 3.00 | 2.83E-09 | 3.00 | 1.62E-08 | 3.00 |

**2.2. Two-dimensional case.** In this section, we will consider the following two-dimensional problem

$$\begin{cases} u_t + u_x + u_y = 0, & x, y \in [0,1] \\ u(0,y,t) = Au(1,y,t) \\ u(x,0,t) = u(x,1,t). \end{cases} \tag{2.21}$$

Without loss of generality, we also choose $A = 2$ to simplify the discussion in the subsequent subsections. Notice that the transfer type boundary condition only acts in the $x$-direction, which simplifies our analysis below somewhat. However this is not essential, the same analysis can be carried out when the transfer type boundary condition is applied in both directions.

**2.2.1. Well-posedness.** Again we will first discuss the well-posedness of the problem. We multiply the partial differential equation in (2.21) by $(1+k_0x)u(x,y,t)$ and integrate over the domain $D_0 = [0,1]^2$. Taking advantage of the boundary conditions, and taking $k_0 = 3$ to cancel the boundary terms generated through integration by parts in the $x$-direction, we obtain

$$0 = \frac{1}{2}\frac{d}{dt}\int_0^1\int_0^1 (1+3x)u^2 dxdy - \frac{3}{2}\int_0^1\int_0^1 u^2 dxdy.$$

Thus,

$$\frac{d}{dt}\int_{D_0}(1+3x)u^2 dxdy = 3\int_{D_0} u^2 dxdy \le 3\int_{D_0}(1+3x)u^2 dxdy.$$

With the Gronwall inequality, we can deduce that

$$\int_{D_0}(1+3x)u^2 dxdy \le \mathrm{e}^{3t}\int_{D_0}(1+3x)u^2 dxdy. \tag{2.22}$$

Therefore, this problem is well-posed under both the weighted norm and the standard $L^2$ norm for fixed time.

**2.2.2. Stability for the semi-discrete DG scheme.** Next, we will discuss the semi-discrete DG scheme for this model and its stability. We define

$$\begin{gathered}0 = x_{\frac{1}{2}} < x_{\frac{3}{2}} < \cdots < x_{n_x+\frac{1}{2}} = 1, \quad h_x = \tfrac{1}{n_x}, \quad I_i = [x_{i-\frac{1}{2}}, x_{i+\frac{1}{2}}],\\ 0 = y_{\frac{1}{2}} < y_{\frac{3}{2}} < \cdots < y_{n_y+\frac{1}{2}} = 1, \quad h_y = \tfrac{1}{n_y}, \quad J_j = [y_{j-\frac{1}{2}}, y_{j+\frac{1}{2}}],\\ h = \max(h_x, h_y), \quad K_{ij} = I_i \times J_j, \quad V_h = \{v : v\,|_{I_{ij}} \in P^k(K_{ij}) \quad or \quad Q^k(K_{ij})\},\end{gathered}$$

where $P^k(K_{ij})$ again denotes the set of polynomials defined on $K_{ij}$ of degree at most $k$ and $Q^k(K_{ij})$ denotes the set of tensor product polynomials defined on $K_{ij}$, namely each member in $Q^k(K_{ij})$ is a polynomial of degree at most $k$ in $x$ for fixed $y$ and is a polynomial of degree at most $k$ in $y$ for fixed $x$. As before, we will consider uniform mesh for simplicity.

The semi-discrete DG scheme can be defined as follows. Find $u_h \in V_h$ such that, for $1 \le i \le n_x, 1 \le j \le n_y$ and all $v_h \in V_h$ we have

(2.23)
$$\begin{aligned}&\int_{K_{ij}} (u_h)_t v_h dxdy - \int_{K_{ij}} u_h (v_h)_x dxdy + \int_{J_j} \left(\widehat{u}_{i+\frac{1}{2},j}(y) v_h(x^-_{i+\frac{1}{2}}, y) - \widehat{u}_{i-\frac{1}{2},j}(y) v_h(x^+_{i-\frac{1}{2}}, y)\right) dy\\ &- \int_{K_{ij}} u_h (v_h)_y dxdy + \int_{I_i} \left(\widehat{u}_{i,j+\frac{1}{2}}(x) v_h(x, y^-_{j+\frac{1}{2}}) - \widehat{u}_{i,j-\frac{1}{2}}(x) v_h(x, y^+_{j+\frac{1}{2}})\right) dx = 0,\end{aligned}$$

wherein

$$\begin{aligned}&\widehat{u}_{i+\frac{1}{2},j}(y) = u_h(x^-_{i+\frac{1}{2}}, y), \quad i = 1, 2, \cdots, n_x, \qquad \widehat{u}_{\frac{1}{2},j}(y) = 2\widehat{u}_{n_x+\frac{1}{2},j}(y),\\ &\widehat{u}_{i,j+\frac{1}{2}}(x) = u_h(x, y^-_{j+\frac{1}{2}}), \quad j = 1, 2, \cdots, n_y, \qquad \widehat{u}(x, y_{\frac{1}{2}}) = \widehat{u}(x, y_{n_y+\frac{1}{2}}).\end{aligned}$$

**Proposition 3.** *For both $P^k$ and $Q^k$ finite element spaces, the DG scheme (2.23) is stable for fixed time $t$,*

$$\|u_h(\cdot,\cdot,t)\|_{L^2(D_0)} \le M_0 \|u_h(\cdot,\cdot,0)\|_{L^2(D_0)}, \tag{2.24}$$

*where $M_0$ is a constant which may depend on $t$.*

*Proof.* Following the procedure in section 2.1.2, let $w = (1+3x)u_h$ and $P$ denote the standard $L^2$ projection to $V_h$, which for the specific $w$ acts in the $x$-direction only. Let $\xi = \frac{2(x-x_i)}{h_x}$ and $\eta = \frac{2(y-y_j)}{h_y}$ in $K_{ij}$. We can express $u_h$ on $K_{ij}$ by

$$u_h(x,y) = \sum_{s=0}^{k} b_s^{ij}(\eta) Q_s(\xi),$$

where $Q_s$ is the scaled Legendre polynomial defined in the previous section, and $b_s^{ij}(\eta)$ is a polynomial of $\eta$ with degree not exceeding $(k-s)$ for $P^k$ and not exceeding $k$ for $Q^k$. Especially for $P^k$ space, we can write the coefficient $b_s^{ij}(\eta)$ as $\sum_{l=0}^{k-s} \beta_s^{ij}(l) Q_l(\eta)$, wherein $\beta_s^{ij}(l)$ are constants. Recall $w = (1+3x)u_h = \left((1+3x_i) + \frac{3h_x}{2}\xi\right) u_h$. With Lemma 2.1, in $K_{ij}$, we have

(2.25)
$$\epsilon^{ij} = w - Pw = \begin{cases} \frac{3}{2}h_x \sum_{s=0}^{k} \beta_s^{ij}(k-s) \sqrt{\frac{(s+1)^2}{(2s+1)(2s+3)}} Q_{k-s}(\eta) Q_{s+1}(\xi), & for\ P^k\ space,\\ \frac{3}{2}h_x b_k^{ij}(\eta) \sqrt{\frac{(k+1)^2}{(2k+1)(2k+3)}} Q_{k+s}(\xi), & for\ Q^k\ space.\end{cases}$$

Take $v_h = Pw$ in the scheme (2.23). Integrate by parts for the second and fourth terms, then use the property of the projection, we have

(2.26)
$$\begin{aligned}&\int_{K_{ij}} (u_h)_t w dxdy + \int_{K_{ij}} (u_h)_x w dxdy + \int_{J_j} \left(u_h(x^+_{i-\frac{1}{2}}, y) - \widehat{u}_{i-\frac{1}{2},j}(y)\right) Pw(x^+_{i-\frac{1}{2}}, y) dy\\ &+ \int_{K_{ij}} (u_h)_y w dxdy + \int_{I_i} \left(u_h(x, y^+_{j-\frac{1}{2}}) - \widehat{u}_{i,j-\frac{1}{2}}(x)\right) Pw(x, y^+_{j-\frac{1}{2}}) dx = 0\end{aligned}$$

Notice also

$$\int_{K_{ij}}(u_h)_x w dxdy = \int_{J_j}\left(\tfrac{1}{2}u_h^2(x^-_{i+\frac{1}{2}},y)(1+3x_{i+\frac{1}{2}}) - \tfrac{1}{2}u_h^2(x^+_{i-\frac{1}{2}},y)(1+3x_{i-\frac{1}{2}})\right)dy - \tfrac{3}{2}\int_{K_{ij}}u_h^2 dxdy,$$
$$\int_{K_{ij}}(u_h)_y w dxdy = \int_{I_i}(1+3x)\left(\tfrac{1}{2}u_h^2(x,y^-_{j+\frac{1}{2}}) - \tfrac{1}{2}u_h^2(x,y^+_{j-\frac{1}{2}})\right)dx.$$

Substituting the two equations above and $Pw = w - \epsilon^{ij}$ into equation (2.26), and noticing that

$$\begin{aligned} u_h(x^-_{i+\frac{1}{2}},y) &= \widehat{u}_{i+\frac{1}{2},j}(y), \qquad for \quad i = 1,2,\cdots,n_x,\\ u_h(x,y^-_{j+\frac{1}{2}}) &= \widehat{u}_{i,j+\frac{1}{2}}(x), \qquad for \quad j = 1,2,\cdots,n_y, \end{aligned}$$

we can sum over $i$ from 1 to $n_x$ and $j$ from 1 to $n_y$ to obtain, with the boundary conditions $\widehat{u}_{\frac{1}{2},j}(y) = 2\widehat{u}_{n_x+\frac{1}{2},j}(y)$ and $\widehat{u}_{i,\frac{1}{2}}(x) = \widehat{u}_{i,n_y+\frac{1}{2}}(x)$,

$$\begin{aligned} &\textstyle\sum_{i=1}^{n_x}\int_{J_j}\frac{1}{2}\widehat{u}^2_{i+\frac{1}{2},j}(y)(1+3x_{i+\frac{1}{2}})dy = \sum_{i=1}^{n_x}\int_{J_j}\frac{1}{2}\widehat{u}^2_{i-\frac{1}{2},j}(y)(1+3x_{i-\frac{1}{2}})dy,\\ &\textstyle\sum_{j=1}^{n_y}\int_{I_i}(1+3x)\left(\frac{1}{2}\widehat{u}^2_{i,j+\frac{1}{2}}(x)\right)dx = \sum_{j=1}^{n_y}\int_{I_i}(1+3x)\left(\frac{1}{2}\widehat{u}^2_{i,j-\frac{1}{2}}(x)\right)dx. \end{aligned}$$

The equation (2.26) now becomes

$$\begin{aligned} 0 = \;& \tfrac{1}{2}\tfrac{d}{dt}\textstyle\int_{D_0}(1+3x)u_h^2 dxdy + \sum_{i,j}\int_{J_j}\frac{1}{2}\left(\widehat{u}^2_{i-\frac{1}{2},j}(y) - u_h^2(x^+_{i-\frac{1}{2}},y)\right)(1+3x_{i-\frac{1}{2}})dy\\ & -\tfrac{3}{2}\textstyle\int_{D_0}u_h^2 dxdy + \sum_{i,j}\int_{J_j}\left(u_h(x^+_{i-\frac{1}{2}},y) - \widehat{u}_{i-\frac{1}{2},j}(y)\right)u_h(x^+_{i-\frac{1}{2}},y)(1+3x_{i-\frac{1}{2}})dy\\ & +\textstyle\sum_{i,j}\int_{I_i}(1+3x)\left(\frac{1}{2}\widehat{u}^2_{i,j-\frac{1}{2}}(x) - \frac{1}{2}u_h^2(x,y^+_{j-\frac{1}{2}})\right)dx\\ & +\textstyle\sum_{i,j}\int_{I_i}(1+3x)\left(u_h(x,y^+_{j-\frac{1}{2}}) - \widehat{u}_{i,j-\frac{1}{2}}(x)\right)u_h(x,y^+_{j-\frac{1}{2}})dx\\ & -\textstyle\sum_{i,j}\int_{J_j}\left(u_h(x^+_{i-\frac{1}{2}},y) - \widehat{u}_{i-\frac{1}{2},j}(y)\right)\epsilon^{ij}(x^+_{i-\frac{1}{2}},y)dy\\ & -\textstyle\sum_{i,j}\int_{I_i}\left(u_h(x,y^+_{j-\frac{1}{2}}) - \widehat{u}_{i,j-\frac{1}{2}}(x)\right)\epsilon^{ij}(x,y^+_{j-\frac{1}{2}})dx\\ = \;& \tfrac{1}{2}\tfrac{d}{dt}\textstyle\int_{D_0}(1+3x)u_h^2 dxdy - \frac{3}{2}\int_{D_0}u_h^2 dxdy\\ & +\textstyle\sum_{i,j}\int_{J_j}\frac{1}{2}\left(u_h(x^+_{i-\frac{1}{2}},y) - \widehat{u}_{i-\frac{1}{2},j}(y)\right)^2(1+3x_{i-\frac{1}{2}})dy\\ & +\textstyle\sum_{i,j}\int_{I_i}\frac{1}{2}(1+3x)\left(u_h(x,y^+_{j-\frac{1}{2}}) - \widehat{u}_{i,j-\frac{1}{2}}(x)\right)^2 dx\\ & -\textstyle\sum_{i,j}\int_{J_j}\left(u_h(x^+_{i-\frac{1}{2}},y) - \widehat{u}_{i-\frac{1}{2},j}(y)\right)\epsilon^{ij}(x^+_{i-\frac{1}{2}},y)dy\\ & -\textstyle\sum_{i,j}\int_{I_i}\left(u_h(x,y^+_{j-\frac{1}{2}}) - \widehat{u}_{i,j-\frac{1}{2}}(x)\right)\epsilon^{ij}(x,y^+_{j-\frac{1}{2}})dx. \end{aligned}$$

Therefore

$$\begin{aligned} & \tfrac{1}{2}\tfrac{d}{dt}\textstyle\int_{D_0}(1+3x)u_h^2 dxdy - \frac{3}{2}\int_{D_0}u_h^2 dxdy\\ \leq\;& \tfrac{1}{2}\textstyle\sum_{i,j}\int_{J_j}\left(\epsilon^{ij}(x^+_{i-\frac{1}{2}},y)\right)^2 dy + \frac{1}{2}\sum_{i,j}\int_{I_i}\left(\epsilon^{ij}(x,y^+_{j-\frac{1}{2}})\right)^2 dx. \end{aligned} \tag{2.27}$$

From the expression of $\epsilon^{ij}$ in (2.25) and the expression of $u_h$, for $P^k$ space, we have

$$\begin{aligned} &\tfrac{1}{2}\textstyle\int_{J_j}\left(\epsilon^{ij}(x^+_{i-\frac{1}{2}},y)\right)^2 dy = \frac{9}{32}h_x^2 h_y\sum_{s=0}^k(\beta_s^{ij}(k-s))^2\frac{1}{2s+1} \leq \frac{9}{32}h_x^2h_y\sum_{s=0}^k(\beta_s^{ij}(k-s))^2,\\ &\tfrac{1}{2}\textstyle\int_{I_i}\left(\epsilon^{ij}(x,y^+_{j-\frac{1}{2}})\right)^2 dx = \frac{9}{32}h_x^3\sum_{s=0}^k(\beta_s^{ij}(k-s))^2\frac{(s+1)^2}{(2s+1)(2s+3)}(2(k-s)+1) \leq \frac{3}{32}(2k+1)h_x^2\sum_{s=0}^k(\beta_s^{ij}(k-s))^2,\\ &\textstyle\int_{K_{ij}}u_h^2 dxdy = \frac{h_xh_y}{4}\sum_{s=0}^k\sum_{l=0}^{k-s}(\beta_s^{ij}(l))^2 \geq \frac{h_xh_y}{4}\sum_{s=0}^k(\beta_s^{ij}(k-s))^2. \end{aligned}$$

For $Q^k$ space, we have

$$\begin{aligned}
&\tfrac{1}{2}\int_{J_j}\left(\epsilon^{ij}(x^+_{i-\frac{1}{2}},y)\right)^2 dy = \tfrac{9}{32}\tfrac{(k+1)^2}{2k+1}h_x^2 h_y \int_{-1}^{1}(b_k^{ij}(\eta))^2 d\eta,\\
&\tfrac{1}{2}\int_{I_i}\left(\epsilon^{ij}(x,y^+_{j-\frac{1}{2}})\right)^2 dx = \tfrac{9}{16}\tfrac{(k+1)^2}{(2k+1)(2k+3)}h_x^3 (b_k^{ij}(-1))^2,\\
&\int_{K_{ij}} u_h^2 dxdy = \tfrac{h_x h_y}{4}\int_{-1}^{1}\textstyle\sum_{s=0}^{k}(b_s^{ij}(\eta))^2 d\eta \geq \tfrac{h_x h_y}{4}\int_{-1}^{1}(b_k^{ij}(\eta))^2 d\eta.
\end{aligned}$$

So for $P^k$ space, we have

$$\begin{aligned}
&\tfrac{1}{2}\textstyle\sum_{i,j}\int_{J_j}\left(\epsilon^{ij}(x^+_{i-\frac{1}{2}},y)\right)^2 dy + \tfrac{1}{2}\sum_{i,j}\int_{I_i}\left(\epsilon^{ij}(x,y^+_{j-\frac{1}{2}})\right)^2 dx\\
=\ &\textstyle\sum_{i,j}\left(\tfrac{9}{32}h_x^2 h_y + \tfrac{3}{32}(2k+1)h_x^3\right)\sum_{s=0}^{k}(\beta_s^{ij}(k-s))^2\\
\leq\ &\textstyle\sum_{i,j}\tfrac{3}{8}\left(3+(2k+1)\tfrac{h_x}{h_y}\right)h_x\int_{K_{ij}}u_h^2 dxdy\\
=\ &\tfrac{3}{8}\left(3+(2k+1)\tfrac{h_x}{h_y}\right)h_x\int_{D_0}u_h^2 dxdy.
\end{aligned}\tag{2.28}$$

If $\frac{h_x}{h_y}$ is upper-bounded by a constant $\alpha$ during refinement (a standard requirement for regular meshes), let $C_k = \frac{3}{8}(3+(2k+1)\alpha)$, then

$$\frac{d}{dt}\int_{D_0}(1+3x)u_h^2 dxdy \leq (3+C_k h_x)\int_{D_0}u_h^2 dxdy \leq (3+C_k h_x)\int_{D_0}(1+3x)u_h^2 dxdy. \tag{2.29}$$

From the Gronwall inequality, we have

$$\int_{D_0}(1+3x)u_h^2(x,y,t)dxdy \leq \mathrm{e}^{(3+C_k h_x)t}\int_{D_0}(1+3x)u_h^2(x,y,0)dxdy.$$

Since this weighted norm is equivalent to the standard $L^2$ norm, we have proved that the semi-discrete DG scheme is stable under the $L^2$ norm for fixed time.

This stability result also holds for the tensor-product polynomial $Q^k$ space. In this case, the coefficient $b_k^{ij}(\eta)$ is a polynomial of degree at most $k$. So with trace theorem, we have $(b_k^{ij}(-1))^2 \leq C_2\int_{-1}^{1}(b_k^{ij}(\eta))^2 d\eta$, wherein $C_2$ is a positive constant. This leads to

$$\begin{aligned}
&\tfrac{1}{2}\textstyle\sum_{i,j}\int_{J_j}\left(\epsilon^{ij}(x^+_{i-\frac{1}{2}},y)\right)^2 dy + \tfrac{1}{2}\sum_{i,j}\int_{I_i}\left(\epsilon^{ij}(x,y^+_{j-\frac{1}{2}})\right)^2 dx\\
=\ &\textstyle\sum_{i,j}\tfrac{9}{32}\tfrac{(k+1)^2}{2k+1}h_x^2 h_y\int_{-1}^{1}(b_k^{ij}(\eta))^2 d\eta + \sum_{i,j}\tfrac{9}{16}\tfrac{(k+1)^2}{(2k+1)(2k+3)}h_x^3(b_k^{ij}(-1))^2\\
\leq\ &\tfrac{9}{16}\tfrac{(k+1)^2}{2k+1}\textstyle\sum_{i,j}\left(\frac{1}{2}h_x^2 h_y + \frac{C_2}{2k+3}h_x^3\right)\frac{4}{h_x h_y}\int_{K_{ij}}u_h^2 dxdy\\
=\ &\tfrac{9}{8}\tfrac{(k+1)^2}{2k+1}\left(1+\tfrac{2C_2}{2k+3}\tfrac{h_x}{h_y}\right)h_x\int_{D_0}u_h^2 dxdy.
\end{aligned}\tag{2.30}$$

So similarly we can get the stability.
□

**2.2.3. Convergence for the semi-discrete DG scheme.** We now consider the error estimate for the DG scheme defined in equation (2.23).

**Proposition 4.** *The solution $u_h$ of the DG scheme (2.23) for the problem (2.21) with the exact solution $u$ smooth enough (namely it is in the Sobolev space $H^{k+1}(D_0)$) satisfies the following error estimate*

$$\begin{aligned}
&\|(u-u_h)(\cdot,\cdot,t)\|_{L^2(D_0)} \leq C_0 h^k, && \text{for the } P^k \text{ space},\\
&\|(u-u_h)(\cdot,\cdot,t)\|_{L^2(D_0)} \leq C_0 h^{k+1}, && \text{for the } Q^k \text{ space},
\end{aligned}\tag{2.31}$$

*where $C_0$ depends on $u$ and its derivatives but is independent of $h$.*

*Proof.* The exact solution also satisfies the scheme (2.23):

(2.32)
$$\begin{aligned}&\int_{K_{ij}} u_t v_h dxdy - \int_{K_{ij}} u(v_h)_x dxdy + \int_{J_j} \left(\widehat{u}_{i+\frac{1}{2},j}(y) v_h(x^-_{i+\frac{1}{2}}, y) - \widehat{u}_{i-\frac{1}{2},j}(y) v_h(x^+_{i-\frac{1}{2}}, y)\right) dy\\ &- \int_{K_{ij}} u(v_h)_y dxdy + \int_{I_i} \left(\widehat{u}_{i,j+\frac{1}{2}}(x) v_h(x, y^-_{j+\frac{1}{2}}) - \widehat{u}_{i,j-\frac{1}{2}}(x) v_h(x, y^+_{j+\frac{1}{2}})\right) dx = 0, \quad \forall v_h \in V_h,\end{aligned}$$

wherein

$$\begin{aligned}&\widehat{u}_{i+\frac{1}{2},j}(y) = u(x^-_{i+\frac{1}{2}}, y) = u(x^+_{i+\frac{1}{2}}, y), \qquad i = 1, 2, \cdots, n_x - 1,\\ &\widehat{u}_{i,j+\frac{1}{2}}(x) = u(x, y^-_{j+\frac{1}{2}}) = u(x, y^+_{j+\frac{1}{2}}), \qquad j = 1, 2, \cdots, n_y - 1,\\ &\widehat{u}_{n_x+\frac{1}{2},j}(y) = u(x^-_{n_x+\frac{1}{2}}, y), \qquad \widehat{u}_{i,n_y+\frac{1}{2}}(x) = u(x, y^-_{n_y+\frac{1}{2}}),\\ &\widehat{u}_{\frac{1}{2},j}(y) = u(x^+_{\frac{1}{2}}, y) = 2\widehat{u}_{n_x+\frac{1}{2},j}(y), \quad \widehat{u}(x, y_{\frac{1}{2}}) = u(x, y^+_{\frac{1}{2}}) = \widehat{u}(x, y_{n_y+\frac{1}{2}}).\end{aligned}$$

Let $e = u - u_h$ denote the error. Subtracting equation (2.23) from (2.32), we can get the error equation

(2.33)
$$\begin{aligned}&\int_{K_{ij}} e_t v_h dxdy - \int_{K_{ij}} e(v_h)_x dxdy + \int_{J_j} \left(\widehat{e}_{i+\frac{1}{2},j}(y) v_h(x^-_{i+\frac{1}{2}}, y) - \widehat{e}_{i-\frac{1}{2},j}(y) v_h(x^+_{i-\frac{1}{2}}, y)\right) dy\\ &- \int_{K_{ij}} e(v_h)_y dxdy + \int_{I_i} \left(\widehat{e}_{i,j+\frac{1}{2}}(x) v_h(x, y^-_{j+\frac{1}{2}}) - \widehat{e}_{i,j-\frac{1}{2}}(x) v_h(x, y^+_{j+\frac{1}{2}})\right) dx = 0, \quad \forall v_h \in V_h,\end{aligned}$$

wherein

$$\begin{aligned}&\widehat{e}_{i+\frac{1}{2},j}(y) = e(x^-_{i+\frac{1}{2}}, y), \qquad i = 1, 2, \cdots, n_x, \qquad \widehat{e}_{\frac{1}{2},j}(y) = 2\widehat{e}_{n_x+\frac{1}{2},j}(y),\\ &\widehat{e}_{i,j+\frac{1}{2}}(x) = e(x, y^-_{j+\frac{1}{2}}), \qquad j = 1, 2, \cdots, n_y, \qquad \widehat{e}(x, y_{\frac{1}{2}}) = \widehat{e}(x, y_{n_y+\frac{1}{2}}).\end{aligned}$$

First consider the $P^k$ space. Let $e_h = u_h - Pu$, $\varepsilon_h = u - Pu$, wherein $P$ is again the standard $2D$ $L^2$ projection onto $P^k(K_{ij})$. Substituting $e = \varepsilon_h - e_h$ into equation (2.33), we can obtain that

(2.34)
$$\begin{aligned}&\int_{K_{ij}} (e_h)_t v_h dxdy - \int_{K_{ij}} (e_h)(v_h)_x dxdy + \int_{J_j} \left((\widehat{e_h})_{i+\frac{1}{2},j}(y) v_h(x^-_{i+\frac{1}{2}}, y) - (\widehat{e_h})_{i-\frac{1}{2},j}(y) v_h(x^+_{i-\frac{1}{2}}, y)\right) dy\\ &- \int_{K_{ij}} (e_h)(v_h)_y dxdy + \int_{I_i} \left((\widehat{e_h})_{i,j+\frac{1}{2}}(x) v_h(x, y^-_{j+\frac{1}{2}}) - (\widehat{e_h})_{i,j-\frac{1}{2}}(x) v_h(x, y^+_{j+\frac{1}{2}})\right) dx\\ =\ &\int_{K_{ij}} (\varepsilon_h)_t v_h dxdy - \int_{K_{ij}} (\varepsilon_h)(v_h)_x dxdy + \int_{J_j} \left((\widehat{\varepsilon_h})_{i+\frac{1}{2},j}(y) v_h(x^-_{i+\frac{1}{2}}, y) - (\widehat{\varepsilon_h})_{i-\frac{1}{2},j}(y) v_h(x^+_{i-\frac{1}{2}}, y)\right) dy\\ &- \int_{K_{ij}} (\varepsilon_h)(v_h)_y dxdy + \int_{I_i} \left((\widehat{\varepsilon_h})_{i,j+\frac{1}{2}}(x) v_h(x, y^-_{j+\frac{1}{2}}) - (\widehat{\varepsilon_h})_{i,j-\frac{1}{2}}(x) v_h(x, y^+_{j+\frac{1}{2}})\right) dx, \quad \forall v_h \in V_h,\end{aligned}$$

wherein

$$\begin{aligned}&(\widehat{e_h})_{i+\frac{1}{2},j}(y) = e_h(x^-_{i+\frac{1}{2}}, y), \qquad i = 1, 2, \cdots, n_x, \qquad (\widehat{e_h})_{\frac{1}{2},j}(y) = 2(\widehat{e_h})_{n_x+\frac{1}{2},j}(y),\\ &(\widehat{e_h})_{i,j+\frac{1}{2}}(x) = e_h(x, y^-_{j+\frac{1}{2}}), \qquad j = 1, 2, \cdots, n_y, \qquad (\widehat{e_h})(x, y_{\frac{1}{2}}) = (\widehat{e_h})(x, y_{n_y+\frac{1}{2}}),\\ &(\widehat{\varepsilon_h})_{i+\frac{1}{2},j}(y) = \varepsilon_h(x^-_{i+\frac{1}{2}}, y), \qquad i = 1, 2, \cdots, n_x, \qquad (\widehat{\varepsilon_h})_{\frac{1}{2},j}(y) = 2(\widehat{\varepsilon_h})_{n_x+\frac{1}{2},j}(y),\\ &(\widehat{\varepsilon_h})_{i,j+\frac{1}{2}}(x) = \varepsilon_h(x, y^-_{j+\frac{1}{2}}), \qquad j = 1, 2, \cdots, n_y, \qquad (\widehat{\varepsilon_h})(x, y_{\frac{1}{2}}) = (\widehat{\varepsilon_h})(x, y_{n_y+\frac{1}{2}}).\end{aligned}$$

Similar to the proof of convergence for the $1D$ case, taking $w = (1 + 3x)e_h$ and $v_h = Pw$, we can use the approach in the stability proof to deal with the left hand side of (2.34), obtaining

$$\sum_{i,j} LHS_{ij} \geq \frac{1}{2}\left(\frac{d}{dt}\int_{D_0} (1 + 3x) e_h^2 dxdy - (3 + C_k h_x)\int_{D_0} e_h^2 dxdy\right).$$

Notice that $v_h$, $(v_h)_x$ and $(v_h)_y$ all belong to the space $P^k(K_{ij})$, with the properties of the $L^2$ projection, the first two terms and the fourth term of the right hand side of (2.34) are equal to 0, hence

$$\begin{aligned} RHS_{ij} = \quad & \int_{J_j} \left( |(\widehat{\varepsilon_h})_{i+\frac{1}{2},j}(y)(Pw)(x^-_{i+\frac{1}{2}},y)| + |(\widehat{\varepsilon_h})_{i-\frac{1}{2},j}(y)(Pw)(x^+_{i-\frac{1}{2}},y)| \right) dy \\ & + \int_{I_i} \left( |(\widehat{\varepsilon_h})_{i,j+\frac{1}{2}}(x)(Pw)(x,y^-_{j+\frac{1}{2}})| + |(\widehat{\varepsilon_h})_{i,j-\frac{1}{2}}(x)(Pw)(x,y^+_{j+\frac{1}{2}})| \right) dx. \end{aligned}$$

We now just consider the first item, as other terms can be handled similarly. Under the requirement for regular mesh, using the trace inequality for $Pw$, we have

$$\begin{aligned} & \int_{J_j} |(\widehat{\varepsilon_h})_{i+\frac{1}{2},j}(y)(Pw)(x^-_{i+\frac{1}{2}},y)|dy \\ \leq \quad & \int_{J_j} \left( \tfrac{1}{h}((\widehat{\varepsilon_h})_{i+\frac{1}{2},j}(y))^2 + h((Pw)(x^-_{i+\frac{1}{2}},y))^2 \right) dy \\ \leq \quad & \tfrac{1}{h}\int_{J_j}((\widehat{\varepsilon_h})_{i+\frac{1}{2},j}(y))^2 dy + C\int_{K_{ij}}(Pw)^2 dxdy \end{aligned}$$

Notice that $\int_{K_{ij}}(Pw)^2 dxdy \leq \int_{K_{ij}} w^2 dxdy \leq 4\int_{K_{ij}}(1+3x)e_h^2 dxdy$. With the approximation property of $\varepsilon_h$, we have

$$\sum_{i,j} RHS_{ij} \leq Ch^{2k} + C\int_{D_0}(1+3x)e_h^2 dxdy,$$

So we have

$$\frac{1}{2}\left( \frac{d}{dt}\int_{D_0}(1+3x)e_h^2 dx - (3+C_k h_x)\int_{D_0} e_h^2 dx \right) \leq Ch^{2k} + C\int_{D_0}(1+3x)e_h^2 dx. \tag{2.35}$$

With a suitable initial condition, Gronwall inequality and equivalence of the two norms, we finally get the sub-optimal $L^2$ error estimate

$$\|(u-u_h)(\cdot,\cdot,t)\|_{L^2(D_0)} \leq C_0 h^k. \tag{2.36}$$

Notice that we are getting a sub-optimal error estimate because we have used the standard $L^2$ projection for $u$ in the proof. Optimal error estimates of $O(h^{k+1})$ can be obtained if the DG space is $Q^k$ instead of $P^k$, since in this case we can replace the $L^2$ projection by a 2D Gauss-Radau type projection (see for example [8, 16]). We will not give the details here to save space. □

**2.2.4. Numerical examples. Example 2.** We test following problem

$$\begin{cases} u_t + u_x + u_y = -\frac{1}{2}\sin(2\pi(x+y-2t)), & x,y \in [0,1], \\ u(0,y,t) = 2u(1,y,t), \\ u(x,0,t) = u(x,1,t) \end{cases}$$

which has the exact solution $u(x,y,t) = \sin(2\pi(x+y-2t))(1-\frac{1}{2}x)$. Using our scheme with $P^2$ elements and third order time discretization, we get the errors and orders of accuracy in Table 2.2. We obtain clearly third order accuracy, indicating that our error estimate is perhaps not sharp for such rectangular meshes.

## 3. A biological model.

TABLE 2.2
*error table,* $t = 0.1$, $cfl = 0.2$

| $N$ | $L^1$-err | $L^1$-ord | $L^2$-err | $L^2$-ord | $L^\infty$-err | $L^\infty$-ord |
|---|---|---|---|---|---|---|
| 10 | 2.11E-03 | – | 3.30E-03 | – | 3.75E-02 | – |
| 20 | 2.64E-04 | 3.00 | 4.17E-04 | 2.99 | 4.81E-03 | 2.96 |
| 40 | 3.29E-05 | 3.01 | 5.23E-05 | 3.00 | 6.13E-04 | 2.97 |
| 80 | 4.11E-06 | 3.00 | 6.54E-06 | 3.00 | 7.69E-05 | 2.99 |
| 160 | 5.13E-07 | 3.00 | 8.17E-07 | 3.00 | 9.64E-06 | 3.00 |

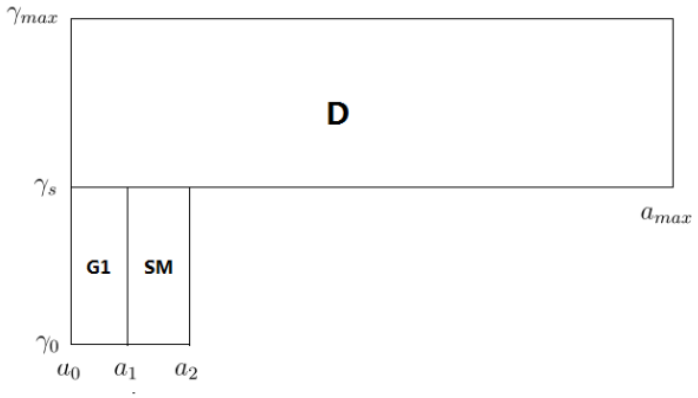


FIG. 3.1. *Fields of the definition for* 3 *cellular phases.*

**3.1. The follicle selection model.** The follicle selection model is a multi-domain model for ovarian follicular development. The development of ovarian follicles is a crucial process for the reproduction in mammals. This model is developed in [18, 17, 14, 1, 2, 15]. In this model, each ovarian follicle is described through a $2D$ density function giving an age and maturity-structured description of its cell population of granulosa cells. The cell population dynamics is ruled by a first-order conservation law with variable coefficients which describes the changes in the granulosa cell age and maturity, and with a source term corresponding to cell apoptosis. The model has the transfer type boundary conditions because of cell mitosis, which means that at the end of a cell cycle, one mother cell gives birth to two daughter cells. In the model, this is described as the density doubling its value at the end of the cell.

There are slight differences among the models discussed in the references listed above, mainly through different partitions of biological domains and expressions of coefficients. We will consider the model in [18] as a representative example. This is a nice example of multi-domain problems with discontinuous flux communication through boundaries. We will first discuss the well-posedness of the problem and then analyze the stability of the related semi-discrete DG scheme. We will omit the error estimates for the semi-discrete DG scheme to save space.

The granulosa cell population consists of proliferating cells (they are running along the cell cycle), differentiated cells (they have left the cell cycle) and apoptotic cells (they have engaged in a dying program). We characterize the cells by their position within or outside the cell cycle and their sensitivity to FSH (follicle stimulating hormone). This leads us to distinguish 3 cellular phases (domains) within the granulosa cell population detailed in [18]. The domains for these three phases are shown in Figure 3.1. We denote the whole domains by $\Omega$.

For a given follicle, we introduce the cell density function $\phi_f(x, y, t)$, wherein the subscript $f = 1, \cdots, F$ represent the serial number of follicles; $t$ denotes time; $x$ denotes the cell age, i.e. its position within the cell cycle, or, if the cell is already differentiated, the sum of the age reached at the cell cycle exit and the time elapsed afterwards; and $y$ is a marker of cell maturity representing the cell responsiveness to FSH [21]. In each biological cellular phase (domain), the cell population dynamics is ruled by a PDE detailed below. In the $G1$, $SM$, and $D$ phase or domain respectively, we have

$$\begin{array}{ll} \frac{\partial \phi_f}{\partial t} + \frac{\partial g_f(u_f)\phi_f}{\partial x} + \frac{\partial h_f(y,u_f)\phi_f}{\partial y} = -\Lambda(y,U)\phi_f, & (x,y) \in G1, \\ \frac{\partial \phi_f}{\partial t} + \frac{\partial \phi_f}{\partial x} = 0, & (x,y) \in SM, \\ \frac{\partial \phi_f}{\partial t} + \frac{\partial \phi_f}{\partial x} + \frac{\partial h_f(y,u_f)\phi_f}{\partial y} = -\Lambda(y,U)\phi_f, & (x,y) \in D, \end{array} \tag{3.1}$$

where the functions $g_f$, $h_f$ and $\Lambda$ are respectively the aging and maturation velocities, and the source term. The $u_f$ and $U$ arguments are respectively the local control term and global control term detailed in [18].

Boundary conditions are given as follows

$$\begin{cases} g_f(u_f)\phi_f(a_0^+, y, t) = 2\phi_f(a_2^-, y, t), & y \in [\gamma_0, \gamma_s], \\ \phi_f(a_1^+, y, t) = g_f(u_f)\phi_f(a_1^-, y, t), & y \in [\gamma_0, \gamma_s], \\ \phi_f(x, \gamma_s^+, t) = \phi_f(x, \gamma_s^-, t), & x \in [a_0, a_1], \\ \phi_f(x, \gamma_0^+, t) = 0, & x \in [a_0, a_2], \\ \phi_f(x, \gamma_0^+, t) = 0, & x \in [a_1, a_{max}], \\ \phi_f(a_0^+, y, t) = 0, & y \in [\gamma_s, \gamma_{max}]. \end{cases} \tag{3.2}$$

Here we define the PDEs in (3.1) together with the boundary conditions in (3.2) as our biological model problem.

We have the following assumptions for the functions $g_f$, $h_f$ and $\Lambda$:

$$\begin{array}{c} 0 < r_1 \le g_f(u_f) \le r_2, \quad \forall\, t, \qquad \Lambda(y,U) \ge 0, \quad \forall\, (y,U), \\ h_f(y,u_f) \ge 0, \quad \|h_f(y,u_f)\|_{L^\infty} \le M_1, \quad \|\frac{\partial h_f(y,u_f)}{\partial y}\|_{L^\infty} \le M_2 \end{array} \tag{3.3}$$

where $r_1$, $r_2$, $M_1$ and $M_2$ are fixed positive constants.

In [18, 2], finite volume schemes were used to solve this problem, with special treatments for discontinuous flux communication, which were much more complicated than the treatments in our RKDG scheme. Also, no stability or convergence proofs were provided for these finite volume schemes.

**3.2. Well-posedness of the problem.** In order to discuss the well-posedness, we let $\omega(x) = 1 + k_0(x - a_0)$, multiply each PDE by $\omega(x)\phi_f(x, y, t)$ and integrate on its own domain. Here $k_0$ is a positive constant, to be determined later.

In the $G1$ domain, we have

$$\begin{aligned} 0 = \; & \int_{G1} \frac{\partial \phi_f}{\partial t}\omega(x)\phi_f dxdy + \int_{G1} \frac{\partial g_f(u_f)\phi_f}{\partial x}\omega(x)\phi_f dxdy \\ & + \int_{G1} \frac{\partial h_f(y,u_f)\phi_f}{\partial y}\omega(x)\phi_f dxdy + \int_{G1} \Lambda(y,U)\omega(x)\phi_f^2 dxdy. \end{aligned}$$

Performing simplification similar to that in the $2D$ case studied in the last section, we can deduce that

$$\begin{aligned} & \tfrac{1}{2}\tfrac{d}{dt}\textstyle\int_{G1} \omega(x)\phi_f^2 dxdy = -\tfrac{1}{2}\int_{\gamma_0}^{\gamma_s} g_f(u_f)\phi_f^2(a_1^-, y, t)(1 + k_0(a_1 - a_0))dy \\ + \; & \tfrac{1}{2}\textstyle\int_{\gamma_0}^{\gamma_s} g_f(u_f)\phi_f^2(a_0^+, y, t)dy + \frac{k_0 g_f(u_f)}{2}\int_{G1}\phi_f^2 dxdy \\ - \; & \tfrac{1}{2}\textstyle\int_{a_0}^{a_1} h_f(\gamma_s, u_f)\omega(x)\phi_f^2(x, \gamma_s^-, t)dx - \frac{1}{2}\int_{G1}\frac{\partial h_f(y,u_f)}{\partial y}\omega(x)\phi_f^2 dxdy \\ - \; & \textstyle\int_{G1}\Lambda(y,U)\omega(x)\phi_f^2 dxdy. \end{aligned} \tag{3.4}$$

The other two domains can be handled similarly. For the $SM$ domain,

$$\begin{aligned}(3.5)\qquad &\tfrac{1}{2}\tfrac{d}{dt}\textstyle\int_{SM}\omega(x)\phi_f^2dxdy = -\tfrac{1}{2}\int_{\gamma_0}^{\gamma_s}\phi_f^2(a_2^-,y,t)(1+k_0(a_2-a_0))dy\\ +\;&\tfrac{1}{2}\textstyle\int_{\gamma_0}^{\gamma_s}\phi_f^2(a_1^+,y,t)(1+k_0(a_1-a_0))dy+\tfrac{k_0}{2}\int_{SM}\phi_f^2dxdy,\end{aligned}$$

and for the $D$ domain,

$$\begin{aligned}(3.6)\qquad &\tfrac{1}{2}\tfrac{d}{dt}\textstyle\int_D\omega(x)\phi_f^2dxdy = \tfrac{k_0}{2}\int_D\phi_f^2dxdy-\tfrac{1}{2}\int_{a_0}^{a_1}h_f(\gamma_s,u_f)\omega(x)\phi_f^2(x,\gamma_s^+,t)dx\\ -\;&\tfrac{1}{2}\textstyle\int_D\frac{\partial h_f(y,u_f)}{\partial y}\omega(x)\phi_f^2dxdy-\int_D\Lambda(y,U)\omega(x)\phi_f^2dxdy.\end{aligned}$$

In order to control the boundary terms, we multiply (3.4), (3.5) and (3.6) by $\alpha_1$, $\alpha_2$ and $\alpha_3$ respectively and then sum them up, where $\alpha_1$, $\alpha_2$ and $\alpha_3$ are positive constants to be determined later. We then substitute the boundary conditions. Let

$$(3.7)\qquad \|\phi_f\|^2_{\alpha,k_0}=\left(\alpha_1\int_{G1}\omega(x)\phi_f^2dxdy+\alpha_2\int_{SM}\omega(x)\phi_f^2dxdy+\alpha_3\int_D\omega(x)\phi_f^2dxdy\right),$$

we have $LHS=\frac{1}{2}\frac{d}{dt}\|\phi_f\|^2_{\alpha,k_0}$ , and

$$\begin{aligned}RHS=\;&-\tfrac{1}{2}\textstyle\int_{\gamma_0}^{\gamma_s}\left(\alpha_1g_f(u_f)-\alpha_2g_f^2(u_f)\right)\phi_f^2(a_1^-,y,t)(1+k_0(a_1-a_0))dy\\ &-\tfrac{1}{2}\textstyle\int_{a_0}^{a_1}(\alpha_1-\alpha_3)h_f(\gamma_s,u_f)\omega(x)\phi_f^2(x,\gamma_s^-,t)dx\\ &-\tfrac{1}{2}\textstyle\int_{\gamma_0}^{\gamma_s}\left(\alpha_2(1+k_0(a_2-a_0))-\alpha_1\frac{4}{g_f(u_f)}\right)\phi_f^2(a_2^-,y,t)dy\\ &-\tfrac{\alpha_1}{2}\textstyle\int_{G1}\left(\frac{\partial h_f(y,u_f)}{\partial y}+2\Lambda(y,U)\right)\omega(x)\phi_f^2dxdy\\ &-\tfrac{\alpha_3}{2}\textstyle\int_D\left(\frac{\partial h_f(y,u_f)}{\partial y}+2\Lambda(y,U)\right)\omega(x)\phi_f^2dxdy\\ &+\tfrac{\alpha_1k_0g_f(u_f)}{2}\textstyle\int_{G1}\phi_f^2dxdy+\frac{\alpha_2k_0}{2}\int_{SM}\phi_f^2dxdy+\frac{\alpha_3k_0}{2}\int_D\phi_f^2dxdy\\ =\;&\mathrm{I}+\mathrm{II}+\mathrm{III},\end{aligned}$$

where I, II and III represent the summation of terms in the first three rows, terms in the next two rows and terms in the last row, respectively.

Noticing the assumptions in (3.3), we have

$$\mathrm{II}\le\frac{M_2}{2}\|\phi_f\|^2_{\alpha,k_0},\qquad \mathrm{III}\le\frac{C_{k_0}}{2}\|\phi_f\|^2_{\alpha,k_0},$$

where $C_{k_0}=k_0\max(1,r_2)$.

To control I to be non-positive, we can first choose a positive number $k_0$ to satisfy $r_2\le\frac{1+k_0(a_2-a_0)}{4}r_1$, then take $\alpha_2=1$, $\alpha_1=\alpha_3$ and $\frac{\alpha_1}{\alpha_2}\in[r_2,\frac{1+k_0(a_2-a_0)}{4}r_1]$, so that

$$(3.8)\qquad\begin{cases}\alpha_1g_f(u_f)-\alpha_2g_f^2(u_f)\ge0,\\ \alpha_1-\alpha_3\ge0,\\ \alpha_2(1+k_0(a_2-a_0))-\alpha_1\frac{4}{g_f(u_f)}\ge0.\end{cases}$$

Thus $\mathrm{I}\le0$, and therefore we have

$$(3.9)\qquad \frac{d}{dt}\|\phi_f\|^2_{\alpha,k_0}\le(M_2+C_{k_0})\|\phi_f\|^2_{\alpha,k_0}.$$

With the Gronwall Lemma and the equivalence of the weighted norm and the standard $L^2$ norm, we can claim that the problem is well-posed for fixed time.

**3.3. Stability for the semi-discrete DG scheme.** Next, we will discuss the semi-discrete DG scheme for this model and its stability. For simplicity, we consider uniform partition.

$$
\begin{aligned}
&a_0 = x_{\frac{1}{2}} < x_{\frac{3}{2}} < \cdots < x_{n_x+\frac{1}{2}} = a_{max}, \quad h_x = \tfrac{a_{max}-a_0}{n_x},\\
&\gamma_0 = y_{\frac{1}{2}} < y_{\frac{3}{2}} < \cdots < y_{n_y+\frac{1}{2}} = \gamma_{max}, \quad h_y = \tfrac{\gamma_{max}-\gamma_0}{n_y},\\
&I_i = [x_{i-\frac{1}{2}}, x_{i+\frac{1}{2}}], \quad J_j = [y_{j-\frac{1}{2}}, y_{j+\frac{1}{2}}], \quad K_{ij} = I_i \times J_j, \quad V_h = \{v : v\mid_{I_{ij}} \in P^k(K_{ij})\}
\end{aligned}
$$

where $P^k(K_{ij})$ again denotes the set of polynomials defined on $K_{ij}$ of degree at most $k$. We assume $n_x$ and $n_y$ are chosen such that there exist positive integers $n_{x_1}$, $n_{x_2}$ and $n_{y_1}$ satisfying

$$x_{n_{x_1}+\frac{1}{2}} = a_1, \quad x_{n_{x_2}+\frac{1}{2}} = a_2, \quad y_{n_{y_1}+\frac{1}{2}} = \gamma_s.$$

The semi-discrete DG scheme can be defined as follows. For a fixed follicle $f$, $f = 1, \cdots, F$, find $\phi_{fh} \in V_h$ such that, for $1 \le i \le n_x, 1 \le j \le n_y$ and all $v_h \in V_h$, we have

(3.10)
$$
\begin{aligned}
&\textstyle\int_{K_{ij}} (\phi_{fh})_t v_h dxdy - \int_{K_{ij}} g_f(u_f)\phi_{fh}(v_h)_x dxdy - \int_{K_{ij}} h_f(y,u_f)\phi_{fh}(v_h)_y dxdy\\
&+\textstyle\int_{J_j} \left(\widehat{g_f\phi_f}_{i+\frac{1}{2},j}(y) v_h(x^-_{i+\frac{1}{2}}, y) - \widehat{g_f\phi_f}_{i-\frac{1}{2},j}(y) v_h(x^+_{i-\frac{1}{2}}, y)\right) dy\\
&+\textstyle\int_{I_i} \left(\widehat{h_f\phi_f}_{i,j+\frac{1}{2}}(x) v_h(x, y^-_{j+\frac{1}{2}}) - \widehat{h_f\phi_f}_{i,j-\frac{1}{2}}(x) v_h(x, y^+_{j+\frac{1}{2}})\right) dx\\
&= -\textstyle\int_{K_{ij}} \Lambda(y,U)\phi_{fh} v_h, \qquad for\ K_{ij} \subset G1,
\end{aligned}
$$

(3.11)
$$
\begin{aligned}
&\textstyle\int_{K_{ij}} (\phi_{fh})_t v_h dxdy - \int_{K_{ij}} \phi_{fh}(v_h)_x dxdy\\
&+\textstyle\int_{J_j} \left(\widehat{\phi_f}_{i+\frac{1}{2},j}(y) v_h(x^-_{i+\frac{1}{2}}, y) - \widehat{\phi_f}_{i-\frac{1}{2},j}(y) v_h(x^+_{i-\frac{1}{2}}, y)\right) dy = 0 \qquad for\ K_{ij} \subset SM,
\end{aligned}
$$

(3.12)
$$
\begin{aligned}
&\textstyle\int_{K_{ij}} (\phi_{fh})_t v_h dxdy - \int_{K_{ij}} \phi_{fh}(v_h)_x dxdy - \int_{K_{ij}} h_f(y,u_f)\phi_{fh}(v_h)_y dxdy\\
&+\textstyle\int_{J_j} \left(\widehat{\phi_f}_{i+\frac{1}{2},j}(y) v_h(x^-_{i+\frac{1}{2}}, y) - \widehat{\phi_f}_{i-\frac{1}{2},j}(y) v_h(x^+_{i-\frac{1}{2}}, y)\right) dy\\
&+\textstyle\int_{I_i} \left(\widehat{h_f\phi_f}_{i,j+\frac{1}{2}}(x) v_h(x, y^-_{j+\frac{1}{2}}) - \widehat{h_f\phi_f}_{i,j-\frac{1}{2}}(x) v_h(x, y^+_{j+\frac{1}{2}})\right) dx\\
&= -\textstyle\int_{K_{ij}} \Lambda(y,U)\phi_{fh} v_h, \qquad for\ K_{ij} \subset D,
\end{aligned}
$$

wherein we take the upwind flux

(3.13)
$$
\begin{aligned}
&\widehat{g_f\phi_f}_{i+\frac{1}{2},j}(y) = g_f(u_f)\phi_{fh}(x^-_{i+\frac{1}{2}}, y), \quad K_{ij} \subset G1,\\
&\widehat{\phi_f}_{i+\frac{1}{2},j}(y) = \phi_{fh}(x^-_{i+\frac{1}{2}}, y), \quad K_{ij} \subset SM \cup D,\\
&\widehat{h_f\phi_f}_{i,j+\frac{1}{2}}(x) = h_f(y_{j+\frac{1}{2}}, u_f)\phi_{fh}(x, y^-_{j+\frac{1}{2}}), \quad K_{ij} \subset G1 \cup D,\\
&\widehat{\phi_f}_{\frac{1}{2},j}(y) = 0, \quad j = n_{y_1}+1, \cdots, n_y,\\
&\widehat{g_f\phi_f}_{\frac{1}{2},j}(y) = 2\widehat{\phi_f}_{n_{x_2}+\frac{1}{2},j}(y), \quad \widehat{\phi_f}_{n_{x_1}+\frac{1}{2},j}(y) = \widehat{g_f\phi_f}_{n_{x_1}+\frac{1}{2},j}(y), \qquad j = 1, 2, \cdots, n_{y_1},\\
&\widehat{h_f\phi_f}_{i,\frac{1}{2}}(x) = 0, \quad i = 1, 2, \cdots, n_{x_1}, \qquad \widehat{h_f\phi_f}_{i,n_{y_1}+\frac{1}{2}}(x) = 0, \quad i = n_{x_1}+1, \cdots, n_x.
\end{aligned}
$$

**Proposition 5.** *Assume that (3.3) hold true, then the DG scheme (3.10), (3.11) and (3.12) with fluxes chosen in (3.13) is stable for fixed time t,*

$$\|\phi_{fh}(\cdot,\cdot,t)\|_{L^2(\Omega)} \le M_0 \|\phi_{fh}(\cdot,\cdot,0)\|_{L^2(\Omega)}, \tag{3.14}$$

*where $M_0$ is a constant which may depend on $t$.*

*Proof.* We can prove the stability for this semi-discrete DG scheme following the steps we used in the previous section for the simple 2D model, and the proof of well-posedness for the biological model. Similar to the proof in section 2.2.2, let $w = \omega(x)\phi_{fh}$. As before, we can express $\phi_{fh}$ on $K_{ij}$ by

$$\phi_{fh}(x,y) = \sum_{s=0}^{k} b_s^{ij}(\eta) Q_s(\xi),$$

where the coefficients $b_s^{ij}(\eta) \in P^{k-s}([-1,1])$ are related to the fixed time $t$ which is omitted in the expression. We can also write coefficient $b_s^{ij}(\eta)$ as $\sum_{l=0}^{k-s} \beta_s^{ij}(l) Q_l(\eta)$. Then, in $K_{ij}$, $w = (1+k_0(x-a_0))\phi_{fh} = \left((1+k_0(x_i-a_0)) + \frac{k_0 h_x}{2}\xi\right)\phi_{fh}$. Using Lemma 2.1, we have

$$\epsilon^{ij} = w - Pw = \frac{k_0}{2} h_x \sum_{s=0}^{k} \beta_s^{ij}(k-s) \sqrt{\frac{(s+1)^2}{(2s+1)(2s+3)}} Q_{k-s}(\eta) Q_{s+1}(\xi). \tag{3.15}$$

Take $v_h = Pw$ in the DG scheme, then integrate by part. Doing summation for all the cells $K_{ij}$ in the $G1$ domain, and taking advantage of boundary conditions, we have

$$\begin{aligned}
& \tfrac{1}{2}\tfrac{d}{dt}\textstyle\int_{G1} \omega(x)\phi_{fh}^2 dxdy - \tfrac{k_0}{2}\int_{G1} g_f(u_f)\phi_{fh}^2 dxdy \\
& + \textstyle\int_{G1} \left(\Lambda(y,U) + \tfrac{1}{2}(h_f(y,u_f))_y\right)\omega(x)\phi_{fh}^2 dxdy \\
\leq\ & - \textstyle\sum_{j=1}^{n_{y_1}} \int_{J_j} \tfrac{1}{2} g_f(u_f)\phi_{fh}^2(a_1^-, y)(1+k_0(a_1-a_0))dy + \sum_{j=1}^{n_{y_1}} \int_{J_j} \tfrac{2}{g_f(u_f)}\phi_{fh}^2(a_2^-, y)dy \\
& - \textstyle\sum_{i=1}^{n_{x_1}} \int_{I_i} \tfrac{1}{2} h_f(\gamma_s, u_f)\omega(x)\phi_{fh}^2(x, \gamma_s^-)dx \\
& + \tfrac{1}{2}\textstyle\sum_{K_{ij}\in G1} \int_{J_j} g_f(u_f)\left(\epsilon^{ij}(x_{i-\frac{1}{2}}^+, y)\right)^2 dy \\
& + \tfrac{1}{2}\textstyle\sum_{K_{ij}\in G1} \int_{I_i} h_f(y_{j-\frac{1}{2}}, u_f)\left(\epsilon^{ij}(x, y_{j-\frac{1}{2}}^+)\right)^2 dx
\end{aligned}$$

Let LT denote the summation of the terms in the last two rows above. Notice the assumptions in (3.3) together with the expression of $\epsilon^{ij}$ in (3.15),

$$\begin{aligned}
LT \leq\ & \tfrac{r_2}{2}\textstyle\sum_{K_{ij}\in G1}\int_{J_j}\left(\epsilon^{ij}(x_{i-\frac{1}{2}}^+, y)\right)^2 dy + \tfrac{M_1}{2}\sum_{K_{ij}\in G1}\int_{I_i}\left(\epsilon^{ij}(x, y_{j-\frac{1}{2}}^+)\right)^2 dx \\
\leq\ & \tfrac{1}{2}\textstyle\sum_{K_{ij}\in G1}\left(r_2\tfrac{k_0^2}{32}h_x^2 h_y + M_1\tfrac{k_0^2}{32}\tfrac{2k+1}{3}h_x^3\right)\sum_{s=0}^{k}(\beta_s^{ij}(k-s))^2 \\
\leq\ & \tfrac{1}{2}\textstyle\sum_{K_{ij}\in G1}\tfrac{k_0^2}{8}(r_2 + M_1\tfrac{2k+1}{3}\tfrac{h_x}{h_y})h_x\int_{K_{ij}}\phi_{fh}^2 dxdy \\
\leq\ & \tfrac{k_0^2}{16}(r_2 + M_1\tfrac{2k+1}{3}\tfrac{h_x}{h_y})h_x\textstyle\int_{G1}\phi_{fh}^2 dxdy.
\end{aligned}$$

With the standard requirement for regular meshes ($\frac{h_x}{h_y} \leq \alpha$), let $C_{1_{k,k_0}} = \frac{k_0^2}{16}(r_2 + \frac{2k+1}{3}M_1\alpha)$, then $LT \leq C_{1_{k,k_0}} h_x \int_{G1}\phi_{fh}^2 dxdy \leq C_{1_{k,k_0}} h_x \int_{G1}\omega(x)\phi_{fh}^2 dxdy$. So we have

$$\begin{aligned}
& \tfrac{1}{2}\tfrac{d}{dt}\textstyle\int_{G1}\omega(x)\phi_{fh}^2 dxdy \leq \tfrac{k_0 r_2}{2}\int_{G1}(\phi_{fh})^2 dad\gamma + \tfrac{M_2}{2}\int_{G1}(\phi_{fh})^2(1+k_0 a)dad\gamma \\
& - \textstyle\sum_{j=1}^{n_{y_1}}\int_{J_j}\tfrac{1}{2}g_f(u_f)\phi_{fh}^2(a_1^-, y)(1+k_0(a_1-a_0))dy + \sum_{j=1}^{n_{y_1}}\int_{J_j}\tfrac{2}{g_f(u_f)}\phi_{fh}^2(a_2^-, \gamma)dy \\
& - \textstyle\sum_{i=1}^{n_{x_1}}\int_{I_i}\tfrac{1}{2}h_f(\gamma_s, u_f)\omega(x)\phi_{fh}^2(x, \gamma_s^-)dx + C_{1_{k,k_0}} h_x\int_{G1}\omega(x)\phi_{fh}^2 dxdy.
\end{aligned} \tag{3.16}$$

Similarly for the domains $SM$ and $D$, we have

$$\begin{aligned}
& \tfrac{1}{2}\tfrac{d}{dt}\textstyle\int_{SM}\omega(x)\phi_{fh}^2 dxdy \leq \tfrac{k_0}{2}\int_{SM}\phi_{fh}^2 dxdy - \sum_{j=1}^{n_{y_1}}\int_{J_j}\tfrac{1}{2}\phi_{fh}^2(a_2^-, y)(1+k_0(a_2-a_0))dy \\
& + \textstyle\sum_{j=1}^{n_{y_1}}\int_{J_j}\tfrac{g_f^2(u_f)}{2}\phi_{fh}^2(a_1^-, y)(1+k_0(a_1-a_0))dy + C_{2_{k,k_0}} h_x\int_{SM}\omega(x)\phi_{fh}^2 dxdy.
\end{aligned} \tag{3.17}$$

$$\begin{aligned}(3.18)\qquad &\tfrac{1}{2}\tfrac{d}{dt}\textstyle\int_D \omega(x)\phi_{fh}^2 dxdy \le \tfrac{k_0}{2}\int_D \phi_{fh}^2 dxdy + \tfrac{M_2}{2}\int_D \omega(x)\phi_{fh}^2 dxdy \\ &+\textstyle\sum_{i=1}^{n_{x_1}}\int_{I_i}\tfrac{1}{2}h_f(\gamma_s,u_f)\omega(x)\phi_{fh}^2(x,\gamma_s^-)dx + C_{3_{k,k_0}}h_x\int_D \omega(x)\phi_{fh}^2 dxdy.\end{aligned}$$

We multiply (3.16), (3.17) and (3.18) by $\alpha_1$, $\alpha_2$ and $\alpha_3$ respectively and then sum them up, so $LHS = \frac{1}{2}\frac{d}{dt}\|\phi_{fh}\|^2_{\alpha,k_0}$, and

$$\begin{aligned} RHS = \quad & -\textstyle\sum_{j=1}^{n_{y_1}}\int_{J_j}\frac{1}{2}(\alpha_1 g_f(u_f) - \alpha_2 g_f^2(u_f))\phi_{fh}^2(a_1^-,y)(1+k_0(a_1-a_0))dy \\ & -\textstyle\sum_{j=1}^{n_{y_1}}\int_{J_j}\frac{1}{2}\phi_{fh}^2(a_2^-,y)\left(\alpha_2(1+k_0(a_2-a_0)) - \alpha_1\frac{4}{g_f(u_f)}\right)dy \\ & -\textstyle\sum_{i=1}^{n_{x_1}}\int_{I_i}\frac{1}{2}(\alpha_1-\alpha_3)h_f(\gamma_s,u_f)\omega(x)\phi_{fh}^2(x,\gamma_s^-)dx \\ & +\frac{\alpha_1 M_2}{2}\int_{G1}\omega(x)\phi_{fh}^2 dxdy + \frac{\alpha_3 M_2}{2}\int_D \omega(x)\phi_{fh}^2 dxdy \\ & +\frac{\alpha_1 k_0 r_2}{2}\int_{G1}\phi_{fh}^2 dxdy + \frac{\alpha_2 k_0}{2}\int_{SM}\phi_{fh}^2 dxdy + \frac{\alpha_3 k_0}{2}\int_D \phi_{fh}^2 dxdy \\ & +\alpha_1 C_{1_{k,k_0}}h_x\int_{G1}\omega(x)\phi_{fh}^2 dxdy + \alpha_2 C_{2_{k,k_0}}h_x\int_{SM}\omega(x)\phi_{fh}^2 dxdy \\ & +\alpha_3 C_{3_{k,k_0}}h_x\int_D \omega(x)\phi_{fh}^2 dxdy \\ = \quad & \mathrm{I}' + \mathrm{II}' + \mathrm{III}', \end{aligned}$$

where I′, II′ and III′ represent the summation of terms in the first three rows, terms in the next two rows and terms in last two rows respectively.

Let $C_{k_0} = k_0\max(1,r_2)$, we have

$$\mathrm{II}' \le \frac{1}{2}(M_2 + C_{k_0})\|\phi_{fh}\|^2_{\alpha,k_0}.$$

Take the same $k_0$ and weights $\alpha_i$ $(i=1,2,3)$ to satisfy the conditions in (3.8), and let $C_{k,k_0} = \max(C_{1_{k,k_0}}, C_{2_{k,k_0}}, C_{3_{k,k_0}})$, we have

$$\mathrm{I}' \le 0, \qquad \mathrm{III}' \le C_{k,k_0}h_x\|\phi_{fh}\|^2_{\alpha,k_0}.$$

Hence

$$(3.19)\qquad \frac{d}{dt}\|\phi_{fh}\|^2_{\alpha,k_0} \le (M + C_{k_0} + 2C_{k,k_0}h_x)\|\phi_{fh}\|^2_{\alpha,k_0}$$

Now, from the Gronwall Lemma and the equivalence of the two norms, we can claim that the semi-discrete DG scheme is stable for fixed time.
□

**3.4. Numerical simulation.** In this section, we consider the example described in section 5 of [2]. There is a slight difference from the model in [18] in that the age of the granulosa cell will not come back to 0 at the end of mitosis. This makes the coefficients different but it does not cause any difficulty to the numerical scheme and simulation.

Let us denote by $F$ the number of follicles in the general case. The cell density $\Phi = (\phi_f)_{f=1,\cdots,F}$ satisfies the following system of equations, for $f = 1,\cdots,F$ :

$$\frac{\partial\phi_f(x,y,t)}{\partial t} + \frac{\partial(g_f(x,y,u_f(t))\phi_f(x,y,t)}{\partial x} + \frac{\partial(h_f(x,y,u_f(t))\phi_f(x,y,t)}{\partial y} = -\Lambda(x,y,U(t))\phi_f(x,y,t)$$

in the computational domain $\Omega$ in the $(x,y)$ plane,

$$\Omega = \{(x,y), \quad 0 \le x \le N_c \times D_c, 0 \le y \le 1\}$$

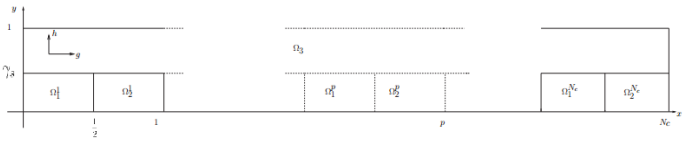

FIG. 3.2. *Computational domain.*

where $N_c$ is the number of cell cycles, $D_c$ is the duration of one cycle and is set to be 1. In consideration of different phases, the whole domain $\Omega$ is divided into 3 parts :

$$\begin{aligned}
\Omega_1^p &= \{(x,y) \in \Omega, \quad (p-1)D_c \le x \le (p-1/2)D_c, \quad 0 \le y \le \gamma_s\}, \\
&\quad p = 1, 2, \cdots, N_c, \quad \Theta_1 = \cup_{p=1}^{N_c} \Omega_1^p, \quad G1 \quad phase, \\
\Omega_2^p &= \{(x,y) \in \Omega, \quad (p-1/2)D_c \le x \le pD_c, \quad 0 \le y \le \gamma_s\}, \\
&\quad p = 1, 2, \cdots, N_c, \quad \Theta_2 = \cup_{p=1}^{N_c} \Omega_2^p, \quad SM \quad phase, \\
\Omega_3 &= \{(x,y) \in \Omega, \quad \gamma_s \le y \le 1\}, \quad D \quad phase,
\end{aligned}$$

which is shown in Figure 3.2.

The aging function $g_f$ is defined by

$$g_f(x,y,u) = \begin{cases} \gamma_1 u + \gamma_2, & for \quad (x,y) \in \Theta_1 \\ 1, & for \quad (x,y) \in \Theta_2 \cup \Omega_3 \end{cases}$$

where $\gamma_1, \gamma_2$ are real positive constants that may depend on the follicle $f$.

The maturation function $h_f$ is defined by

$$h_f(x,y,u) = \begin{cases} \tau_h(-y^2 + (c_1 y + c_2)(1 - \mathrm{e}^{-\frac{u}{\overline{u}}})), & for \quad (x,y) \in \Theta_1 \cup \Omega_3 \\ 0, & for \quad (x,y) \in \Theta_2 \end{cases}$$

where $\tau_h, c_1, c_2$ and $\overline{u}$ are real positive constants that may depend on the follicle f.

The source term, that represents cell loss through apoptosis, is defined by

$$\Lambda(x,y,U) = \begin{cases} \overline{\Lambda} \mathrm{e}^{-\frac{(y-\gamma_s)^2}{\overline{\gamma}}}(1-U), & for \quad (x,y) \in \Theta_1 \cup \Omega_3 \\ 0, & for \quad (x,y) \in \Theta_2 \end{cases}$$

where $\overline{\Lambda}$ and $\overline{\gamma}$ are real positive constants.

Comparing to the general model analyzed before, we have specific expressions for all the coefficients, and the range of the variable $y$ is set to be $[0,1]$. Another difference is that, with the values of constants given below, the coefficient $h_f(x,y,u_f)$ may become negative inside part of the domain $\Omega_3$. In this case, we would need to take the upwinding flux in the scheme. This does not cause any problem to the stability of the scheme.

The equations in the PDE system are coupled together through the argument $u_f(t)$ appearing in the speeds $g_f(x,y,u)$ and $h_f(x,y,u)$ and the argument $U(t)$ appearing in the source term $\Lambda(x,y,U)$. $U(t)$ and $u_f(t)$ represent the plasma FSH level and the locally bioavailable FSH level respectively and depend on the first maturity moment of the densities. If we define

$$m_f(t) = \int_0^1 \int_0^{N_c D_c} y \phi_f(x,y,t) dx dy, \qquad M(t) = \sum_{f=1}^{F} m_f(t),$$

the plasma FSH level $U(t)$ in the arguments of the source term is defined by

$$U(t) = U_{min} + \frac{1 - U_{min}}{1 + \mathrm{e}^{c(M(t) - \overline{M})}},$$

where $U_{min}, c$, and $\overline{M}$ are real positive constants. The locally bioavailable FSH level $u_f(t)$ in the arguments of the speeds is defined by

$$u_f(t) = \min(b_1 + \frac{\mathrm{e}^{b_2 m_f(t)}}{b_3}, 1)U(t) \qquad for \quad f = 1, \cdots, F,$$

where $b_1, b_2$, and $b_3$ are real positive constants that may depend on the follicle $f$. The numerical values of the biological constants are gathered in Table 3.1. To simplify the notation we do not explicitly indicate their possible dependence as a function of the follicle even if it is implied by the $f$ index notation.

TABLE 3.1
Values of the parameters for the biological model simulation. The two follicles in competition differ by the value of $\tau_h$.

| Parameter | Description | Value | |
|---|---|---|---|
| FSH plasma level | | | |
| $U_{min}$ | minimum level | 0.5 | |
| c | slope parameter | 2.0 | |
| $\overline{M}$ | abscissa of the inflection point | 4.5 | |
| apoptosis source term | | | |
| $\overline{\Lambda}$ | intensity factor | 0.1 | |
| $\overline{\gamma}$ | scaling factor | 0.01 | |
| $\gamma_s$ | cellular maturity threshold | 0.3 | |
| intrafollicular FSH level | | | |
| $b_1$ | basal level | 0.08 | |
| $b_2$ | exponential rate | 2.25 | |
| $b_3$ | scaling factor | 1450. | |
| aging function | | | |
| $\gamma_1$ | rate | 1. | |
| $\gamma_2$ | origin | 1. | |
| maturation function | | | |
| $c_1$ | | 0.68 | |
| $c_2$ | | 0.08 | |
| $\overline{u}$ | | 0.02 | |
| $\tau_h$ | | foll.1 | foll.2 |
| | | 0.7 | 1.0 |

The boundary conditions are shown below. For each cell cycle $p$, $p = 1, \cdots, N_c$, the following hold:

- The flux on the $x$-axis is continuous on the interface between $\Omega_1^p$ and $\Omega_2^p$,

$$\phi_f(x^+, y, t) = (\gamma_1 u_f + \gamma_2)\phi_f(x^-, y, t), \quad x = (p - 1/2)D_c, \quad 0 \le y \le \gamma_s.$$

- The flux is doubling at the end of each mitosis cell cycle on the interface between $\Omega_2^p$ and $\Omega_1^{p+1}$,

$$(\gamma_1 u_f + \gamma_2)\phi_f(x^+, y, t) = 2\phi_f(x^-, y, t), \quad x = pD_c, \quad 0 \le y \le \gamma_s.$$

- A waterproof boundary condition holds to the north of the interface between $\Omega_2^p$ and $\Omega_3$,

$$\phi_f(x, \gamma_s^+, t) = 0, \quad (p - 1/2)D_c \le x \le pD_c.$$

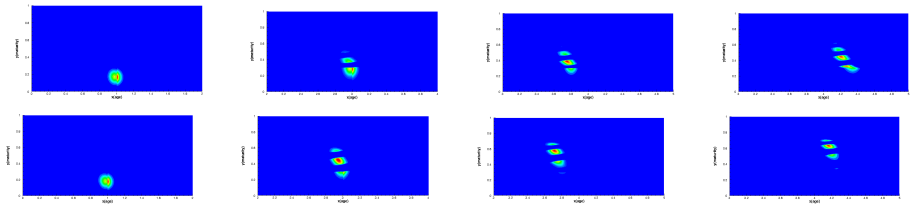

FIG. 3.3. *Full model with the MPP limiter: snapshots of the density at different times of the follicular development for follicle 1(top) and follicle 2(bottom),* $h_x = 0.00625$. *The different colors indicate different levels of cell density. In each line, from left to right, 1st:* $t = 0.66$*; 2nd:* $t = 2.58$*; 3rd:* $t = 3.35$*; 4th:* $t = 3.80$.

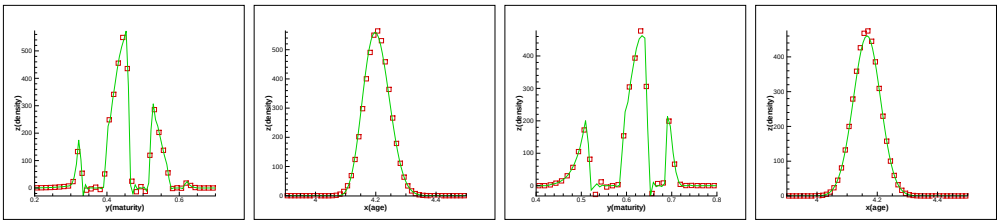


FIG. 3.4. *Comparison of numerical results for the DG method with different* $h_x$*: 0.00625 (solid line) and 0.0125 (symbols) at* $t = 3.80$. *From left to right, 1st: follicle 1 cut at* $x = 4.20$*; 2nd: follicle 1 cut at* $y = 0.45$*; 3rd: follicle 2 cut at* $x = 4.16$*; 4th: follicle 2 cut at* $y = 0.63$.

We refer the readers to [1, 2] and the references therein for more details of this model.

We take $N_c = 5$, and take the initial condition as

$$\phi_f(x, y, 0) = \begin{cases} \frac{1}{2\pi\sigma^2} \mathrm{e}^{-\frac{(x-0.3)^2+(y-0.15)^2}{2\sigma^2}}, & (x, y) \in \Omega_1^1 \\ 0, \quad elsewhere \end{cases}$$

where $\sigma^2 = 0.002$.

The positivity-preserving property for the densities is important. To avoid the mendacious negative oscillation, we follow the framework in a series of papers by Zhang and Shu on high order bound-preserving DG schemes [29, 30], and apply the maximum-principle-preserving (MPP) limiter designed in these papers to our DG scheme. The appearance of the source term in our model can be dealt with, modulo a slight modification of the CFL number. For the 1-$D$ problem, we refer to the details in [20]; the same result can be obtained for the 2-$D$ problem following similar procedure. Notice that it is proved in [29, 30] that such MPP limiters do not affect the high order accuracy of the original DG schemes.

In the numerical results, to illustrate different phenomena at the interfaces, snapshots of the density at significant times of the follicular development are displayed in Figure 3.3. We can see that the structures are resolved quite well in the simulation.

To illustrate the stability of the DG scheme without the MPP limiter, we compare the results for different mesh sizes $h_x$ in Figure 3.4. We can clearly see a grid refinement numerical convergence in these cuts.

To illustrate the effect of the MPP limiter, we compare the cuts of density of the numerical results with and without the MPP limiter in Figure 3.5. We can clearly see that the DG results without the MPP limiter produces negative density, while the results with the MPP limiter is completely positive.

**4. Concluding remarks.** In this paper, we have studied the well-posedness of the PDE and stability and error estimates of the discontinuous Galerkin (DG)

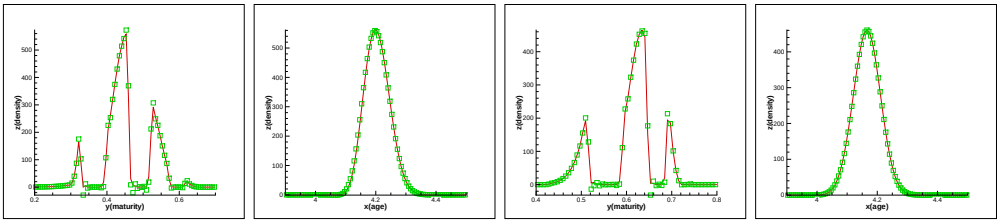

FIG. 3.5. *Comparison for the positivity-preserving property of the numerical results for the DG method with (solid line) and without (symbols) the MPP limiter,* $h_x = 0.00625$, $t = 3.80$. *From left to right, 1st: follicle 1 cut at* $x = 4.20$*; 2nd: follicle 1 cut at* $y = 0.45$*; 3rd: follicle 2 cut at* $x = 4.16$*; 4th: follicle 2 cut at* $y = 0.63$.

method for a class of multi-domain problems with discontinuous flux communication through boundaries. The proof of both well-posedness of the PDE and stability of the DG scheme uses a particular weighted norm, which is equivalent to the regular $L^2$ norm. For the DG method, the particular weight makes the desired test function not in the finite element space, hence a careful study of effect by replacing this test function by its projection into the finite element space has been performed in order to prove stability. The results are first demonstrated through simple one and two-dimensional model problems, then they are generalized to a biological cell proliferation model. Positivity-preserving properties of the DG schemes are also explored. Numerical results, both for the simple one and two-dimensional model problems and for the biological cell proliferation model, are provided to illustrate the good behavior of our DG methods. The schemes and their stability analysis in this paper can be applied to general multi-domain problems with transferring type boundary conditions arising from many applications, for example, in traffic flows, networks, multiphase flows, etc., such generalizations constitute our future work.

## REFERENCES


[1] B. Aymard, F. Clément, F. Coquel and M. Postel, *Numerical simulation of the selection process of the ovarian follicles*, ESAIM: Proceedings, 38, 2012, 99-117.

[2] B. Aymard, F. Clément, F. Coquel and M. Postel, *A numerical method for transport equations with discontinuous flux functions: Application to mathematical modeling of cell dynamics*, SIAM Journal on Scientific Computing, 35, 2013, A2442-A2468.

[3] B. Boutin, F. Coquel and P.G. LeFloch, *Coupling techniques for nonlinear hyperbolic equations. III. The well-balanced approximation of thick interfaces*, SIAM Journal on Numerical Analysis, 51, 2013, 1108-1133.

[4] R. Bürger and K.H. Karlsen, *Conservation laws with discontinuous flux: A short introduction*, Journal of Engineering Mathematics, 60, 2008, 241-247.

[5] R. Bürger, K.H. Karlsen and N.H. Risebro, *A relaxation scheme for continuous sedimentation in ideal clarifier-thickener units*, Computers and Mathematics with Applications, 50, 2005, 993-1009.

[6] R. Bürger, K.H. Karlsen and J.D. Towers, *A conservation law with discontinuous flux modelling traffic flow with abruptly changing road surface conditions*, in Hyperbolic Problems: Theory, Numerics and Applications, Proceedings of Symposia Applied Mathematics, 67, 2009, AMS, Providence, RI, 455-464.

[7] B. Cockburn, S. Hou and C.-W. Shu, *The Runge-Kutta local projection discontinuous Galerkin finite element method for conservation laws IV: the multidimensional case*, Mathematics of Computation, 54, 1990, 545-581.

[8] B. Cockburn, G. Kanschat, I. Perugia and D. Schötzau, *Superconvergence of the local discontinuous Galerkin method for elliptic problems on Cartesian grids*, SIAM Journal on Numerical Analysis, 39, 2001, 264-285.

[9] B. Cockburn, S.-Y. Lin and C.-W. Shu, *TVB Runge-Kutta local projection discontinuous Galerkin finite element method for conservation laws III: one-dimensional systems*, Jour-

nal of Computational Physics, 84, 1989, 90-113.
[10] B. Cockburn and C.-W. Shu, *TVB Runge-Kutta local projection discontinuous Galerkin finite element method for conservation laws II: general framework*, Mathematics of Computation, 52, 1989, 411-435.
[11] B. Cockburn and C.-W. Shu, *The Runge-Kutta discontinuous Galerkin method for conservation laws V: multidimensional systems*, Journal of Computational Physics, 141, 1998, 199-224.
[12] B. Cockburn and C.-W. Shu, *Runge-Kutta discontinuous Galerkin methods for convection-dominated problems*, Journal of Scientific Computing, 16, 2001, 173-261.
[13] P. Ciarlet, *Finite Element Method for Elliptic Problems*, SIAM, Philadelphia, 2002.
[14] F. Clément, *Multiscale modelling of endocrine systems: new insight on the gonadotrope axis*, ESAIM: Proceedings, 27, 2009, 209-226.
[15] F. Clément and D. Monniauxb, *Multiscale modelling of ovarian follicular selection*, Progress in Biophysics and Molecular Biology, 113, 2013, 398-408.
[16] B. Dong and C.-W. Shu, *Analysis of a local discontinuous Galerkin method for linear time-dependent fourth-order problems*, SIAM Journal on Numerical Analysis, 47, 2009, 3240-3268.
[17] N. Echenim, F. Clément and M. Sorine, *Multi-scale modeling of follicular ovulation as a reachability problem*, Multiscale Modeling and Simulation, 6, 2007, 895-912.
[18] N. Echenim, D. Monniaux, M. Sorine and F. Clément, *Multi-scale modeling of the follicle selection process in the ovary*, Mathematical Biosciences, 198, 2005, 57-79.
[19] S. Gottlieb, C.-W. Shu and E. Tadmor, *Strong stability preserving high order time discretization methods*, SIAM Review, 43, 2001, 89-112.
[20] J. Lu, C.-W. Shu and M. Zhang, *Stability analysis and a priori error estimate of explicit Runge-Kutta discontinuous Galerkin methods for correlated random walk with density-dependent turning rates*, Science China Mathematics, 56, 2013, 2645-2676.
[21] J.S. Richards, *Maturation of ovarian follicles: actions and interactions of pituitary and ovarian hormones on follicular cell differentiation*, Physiological Reviews, 60, 1980, 51-89.
[22] W.H. Reed and T.R. Hill, *Triangular mesh methods for the neutron transport equation*, Los Alamos Scientific Laboratory Report LA-UR-73-479, 1973.
[23] N. Seguin and J. Vovelle, *Analysis and approximation of a scalar conservation law with a flux function with discontinuous coefficients*, Mathematical Models and Methods in Applied Sciences, 13, 2003, 221-257.
[24] P. Shang, *Cauchy problem for multiscale conservation laws: Application to structured cell populations*, Journal of Mathematical Analysis and Applications, 401, 2013, 896-920.
[25] C.-W. Shu and S. Osher, *Efficient implementation of essentially non-oscillatory shock-capturing schemes*, Journal of Computational Physics, 77, 1988, 439-471.
[26] J.J. Tyson and B. Novak, *Temporal organization of cell cycle*, Current Biology, 18, 2008, R759-R768.
[27] Q. Zhang and C.-W. Shu, *Error estimates to smooth solutions of Runge-Kutta discontinuous Galerkin methods for scalar conservation laws*, SIAM Journal on Numerical Analysis, 42, 2004, 641-666.
[28] Q. Zhang and C.-W. Shu, *Stability analysis and a priori error estimates of the third order explicit Runge-Kutta discontinuous Galerkin Method for scalar conservation laws*, SIAM Journal on Numerical Analysis, 48, 2010, 1038-1063.
[29] X. Zhang and C.-W. Shu, *On maximum-principle-satisfying high order schemes for scalar conservation laws*, Journal of Computational Physics, 229, 2010, 3091-3120.
[30] X. Zhang and C.-W. Shu, *Positivity-preserving high order finite difference WENO schemes for compressible Euler equations*, Journal of Computational Physics, 231, 2012, 2245-2258.